

Antibody Engineering: Optimizing the Delivery Vehicle

DIANE E. MILENIC

1.1 INTRODUCTION

The progression of monoclonal antibodies (MAbs) for radioimmunotherapy (RIT) has been driven by the need to solve a series of problems. As variants of antibodies have been developed and evaluated in preclinical studies, opportunities and limitations have become evident. Recent advances in DNA technology have led to the ability to tailor and manipulate the immunoglobulin (Ig) molecule for specific functions and *in vivo* properties. This chapter discusses the use of monoclonal antibodies for radiotherapy with an emphasis on the problems that have been encountered and the subsequent solutions.

The exploration of monoclonal antibodies as vehicles for the delivery of radio-nuclides for therapy has been ongoing for almost 50 years (1). In 1948, Pressman and Keighley reported the first *in vivo* use of a radiolabeled antibody for imaging (2). Ten years later, the first report of radiolabeled tumor-specific antibodies was utilized for radioimmunodiagnosis, and in 1960, radiolabeled antibodies were used to selectively deliver a therapeutic dose of radiation to tumor tissue (1, 3). Even at these early stages, investigators were quick to realize the obstacles associated with utilizing antibodies for radioimmunotherapy. Radiation doses delivered to tumors in patients were too low to have significant effects on tumor growth, and the prolonged retention of the radiolabeled antibodies in the blood led to toxicity complications (4). The inherent heterogeneity in specificity and affinity of polyclonal antibodies resulted in *in vivo* variability. The advent of hybridoma technology and the ability to generate mono-specific, monoclonal antibodies produced a resurgence in the use of antibodies as “magic bullets” (5, 6). In the 1980s, the literature exploded with reports of radiolabeled MAbs being evaluated in the clinical setting, initially in radioimmunodiagnostic applications, confirming that MAbs against tumor-associated antigens could target

tumors in patients. Subsequently, RIT clinical trials were initiated to deliver systemically administered radiation to tumors with a specificity that would spare normal tissues from damage (7). This optimistic viewpoint was quickly tempered by the realization of the obstacles inherent to the use of a biological reagent, especially one of xenogeneic origin.

The preclinical and clinical RIT trials exposed the major constraints to the successful clinical use of radiolabeled MAbs: (i) development of human anti-murine immunoglobulin antibodies (HAMA); (ii) inadequate (low) therapeutic levels of radiation doses delivered to tumor lesions; (iii) slow clearance of the radiolabeled MAbs (radioimmunoconjugates) from the blood compartment; (iv) low MAb affinity and avidity; (v) trafficking to, or targeting of, the radioimmunoconjugates to normal organs; and (vi) insufficient penetration of tumor tissue (8, 9). In addition, there were toxicities associated with conjugated radionuclides when the radioimmunoconjugates were metabolized or when the radionuclide dissociated from the immunoconjugate (9). With these problems in mind, a primary focus has been to optimize RIT by manipulating the MAb molecule. As technology permitted, this was initially accomplished with chemical or biochemical techniques to generate a variety of immunoglobulin forms but is now predominated by genetic engineering.

1.2 INTACT MURINE MONOCLONAL ANTIBODIES

In May 2008, a perspective on MAbs by Reichert and Valge-Archer (10) reported that in the periods 1980–1989, 1990–1999, and 2000–2005, 37, 25, and 8 murine MAbs, respectively, were evaluated in the clinic as cancer therapeutics. During this entire 25-year period, radiolabeled MAbs comprised 33% of the murine MAbs (10). To date, only two radiolabeled murine (*mu*) MAbs, both targeting CD20, have received FDA approval. Zevalin, ^{90}Y -rituxan (ibritumomab-tiuxetan), was approved in 2002 and is indicated for relapsed or refractory low-grade follicular transformed non-Hodgkin's lymphoma (NHL). The overall response rate of patients is reported to be 80%; 46% for those with rituximab refractory disease (11). Bexxar (^{131}I -tositumomab) was approved in 2003 for the treatment of non-Hodgkin's B-cell lymphoma in rituximab refractory patients (see Chapter 6). Objective responses following ^{131}I -tositumomab therapy have ranged from 54% to 71% in patients who have undergone previous therapies while for newly diagnosed patients the response rates are 97% with 63% of those experiencing a complete response (12).

In clinical trials using *mu*MAbs for RIT of solid tumors, approximately 73% (ranging from 16% to 100%) of the patients developed HAMA following a single infusion of MAb (13). In contrast, only about 42% of the patients in RIT trials for treatment of hematologic malignancies develop HAMA. When multiple doses of a radioimmunoconjugate have been administered, the amount of MAb that effectively targets tumor tissue is usually compromised after the second administration (13). In general, the human antibody response, especially at earlier time points, is directed against the Fc portion of the MAb molecule (Fig. 1.1). With the passage of time and particularly after repeated infusions, the specificity of the human antibody response

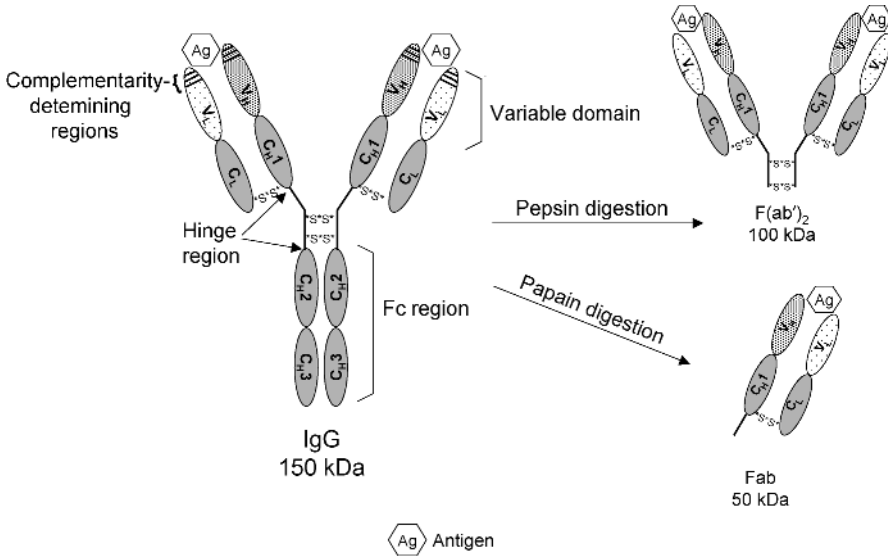


FIGURE 1.1 Schematic of an immunoglobulin structure. Enzymatic digestion of the intact IgG molecule yields $F(ab')_2$ and Fab fragments.

matures and becomes increasingly specific for the variable region of the MAb (13). In some instances, anti-variable region antibodies develop after a single infusion of the MAb (13, 14). This response has the potential of directly inhibiting the ability of the injected MAb from interacting with the targeted tumor (14). As with any therapeutic regimen, for RIT to be effective, multiple treatment cycles will be necessary. Immunomodulatory drugs such as deoxyspergualin, cyclosporin A, or cyclophosphamide have been evaluated as a means of minimizing or suppressing a patient's immune response during RIT (15).

To address these challenges of MAb-directed therapy, several strategies have been employed that center around modifying the MAb molecule. These alterations include reduction in the size of the MAb molecule, deglycosylation, or the addition of side groups. Reduction in size of the MAb molecule has been accomplished through methods such as enzymatic cleavage or genetic engineering (16–18). Digestion of an antibody with pepsin removes the Fc region of the heavy chain on the carboxyl terminus of cysteamine producing $F(ab')_2$ fragments that retain two antigen binding sites and have a molecular weight of ~ 100 kDa (Fig. 1.1). Fab fragments are generated by digestion with papain, an enzyme with a specificity for the amino group of cysteines. In this case, the disulfide bridges between the heavy chains are removed with the Fc region, which results in a molecule ($M_r \sim 50$ kDa) with one antigen binding site. Fab' fragments are produced through reduction and alkylation of $F(ab')_2$, which also yields a MAb molecule with a single antigen binding site and an M_r of ~ 50 kDa (16–18). Comparisons of intact MAbs and $F(ab')_2$ fragments (Fig. 1.1) in RIT clinical trials have demonstrated that the $F(ab')_2$ fragments do have a shorter serum half-life than intact MAbs. Patient antibody responses against $F(ab')_2$ fragments

appear to occur with lower frequency after a single administration of the radioimmunoconjugate. Furthermore, some objective responses to treatment with a radiolabeled $F(ab')_2$ fragment have been observed (19, 20). Autoradiographic studies of radiolabeled MAbs administered to athymic mice bearing human tumor xenografts have illustrated the ability of Fab' and $F(ab')_2$ fragments to penetrate tumor tissue with greater efficiency than intact MAbs (20, 21). The pharmacokinetics of Fab or Fab' fragments is even more rapid than $F(ab')_2$ fragments ($t_{1/2\alpha} \sim 10$ min, $t_{1/2\beta} \sim 1.5$ h for Fab' fragments versus $t_{1/2\alpha} \sim 30$ min, $t_{1/2\beta} \sim 12$ h for $F(ab')_2$ fragments) (22). In general, Fab and Fab' fragments have proven to be less immunogenic than intact MAbs (23). Their greatest disadvantage for RIT applications is their high and persistent renal localization, which appears to be a function of molecular size (22), which greatly increases the risk for renal toxicity. The degree to which the radiolabel is retained in the kidneys depends on the radionuclide and the radiolabeling chemistry (see Chapter 2). Radioiodinated MAbs are rapidly dehalogenated and the radioiodine excreted via the kidneys or into the stomach and intestines. Free radioiodine is trapped in the thyroid gland if there is inadequate blocking with stable iodine. Chelated radiometallonucleides, that is, ^{111}In , ^{90}Y , and ^{177}Lu , are not as readily eliminated from normal tissues when the radioimmunoconjugate is metabolized (24). The retention of radiometals in the kidneys is due to the reabsorption of antibody fragments after their glomerular filtration followed by degradation of the radioimmunoconjugates with trapping of radioactive metabolites within the renal tubular cells (22, 24, 25). Although they are readily eliminated from the body, radioiodines may also pose a concern for toxicity to renal tissue, depending on the dose of radioactivity administered. An effective means of enhancing renal excretion of the radioimmunoconjugates is the blocking of its reabsorption from the luminal fluid in the proximal tubules by administering basic amino acids such as lysine or arginine, prior to or with the radiolabeled MAb fragment (26, 27).

Fragments of MAb that retain immunoreactivity, however, are often difficult to generate (22). As mentioned, they are prepared by proteolytic digestion of intact MAb using enzymes, a procedure that must be optimized for each MAb and usually requires threefold or more MAbs to obtain the final desired quantity of the fragment. The process is inefficient and costly when producing the amounts necessitated by a RIT clinical trial.

1.3 RECOMBINANT IMMUNOGLOBULIN MOLECULES

Antibodies consist of four polypeptide chains, two heavy and two light chains, connected by disulfide bonds; the heavy chains are glycosylated (Fig. 1.1). Several criteria must be met to generate and produce genetically engineered antibodies. First, a host cell is needed that would produce and secrete a properly assembled functional antibody molecule with the appropriate carbohydrate side chains. Second, the DNA must be introduced into the recipient cell in an efficient manner. Finally, expression vectors must be available that permit the expression of the introduced genes as well as the isolation of the cells expressing the introduced antibody genes (28). The vectors

require a plasmid origin for replication, a gene encoding a selectable biochemical phenotype in bacteria and a gene encoding a selectable marker in eukaryotic cells. The creation of recombinant immunoglobulin molecules also requires the transfection of the host cell with two expression vectors, one containing the gene for the heavy chain and the other containing the gene that encodes the light chain.

1.3.1 Chimeric Monoclonal Antibodies

Chimeric MAbs are constructed by ligating the gene encoding the variable region of a murine MAb to the gene encoding the constant region of a human Ig (Fig. 1.2). There are a variety of vectors available into which the murine and human Ig gene sequences can be inserted. In turn, there are a number of expression systems, prokaryotic and eukaryotic, into which the recombinant Ig genes can be introduced and the protein expressed (28, 29). The ability to tailor a MAb of a particular specificity for a certain function broadens the horizon for MAb-directed therapies.

The first clinical trial involving a recombinant/chimeric MAb employed MAb 17-1A, which recognizes the 40 kDa glycoprotein designated epithelial-specific cell adhesion molecule (EpCAM) (30–32). The variable region of MAb 17-1A was fused with a human IgG_{1κ} sequence. Ten patients with metastatic colon carcinoma were given injections of the chimeric (ch) 17-1A. Only one of the patients who received multiple injections developed a low titer antibody response against ch17-1A that was directed against the variable region of the chMAb and not against the human constant domains. In addition, the pharmacokinetics of the ch17-1A was slower than the original murine MAb by sixfold.

Several chMAbs have since been constructed, characterized in preclinical *in vitro* and *in vivo* studies, and have been evaluated in RIT clinical trials. Direct comparisons

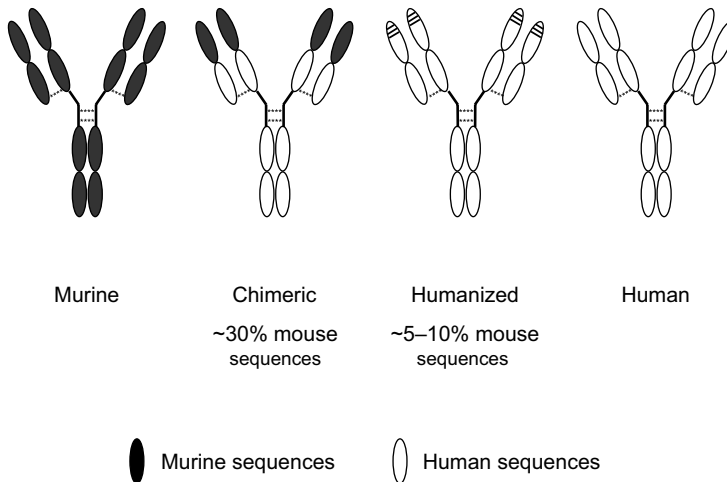


FIGURE 1.2 The “humanization” of the murine IgG to generate forms with increasing percentages of human sequences.

of the chimeric and murine forms of a MAb (B72.3) determined that the chimeric form was quantitatively superior in tumor targeting (33). This enhanced tumor targeting of the chMAB was attributed to its longer plasma half-life, approximately 4.7-fold longer than that of muB72.3. Unfortunately, chMABs have also proven to be immunogenic in patients. Evidence suggests that the degree of immunogenicity may be dependent on the particular MAB. The murine MAb 17-1A elicited antibody responses in 77% of the patients, while the chimeric 17-1A evoked a humoral response in only 5–10% of the patients. In contrast, chB72.3 evoked an antibody response in patients with at least the same frequency as muMAB B72.3 (13). Minimal antibody responses have been reported for patients receiving rituximab, a chimeric anti-CD20 MAB used for non-Hodgkin's B-cell lymphoma; this may be attributed in part to the impaired immune status of these patients (11, 34). The antibody responses appear not as robust as the HAMA responses, and in some cases, more than one dose of chMAB may be administered before an antibody response against the chMAB is elicited. Further humanization of the murine MAB has been accomplished by grafting the complementarity-determining regions (CDRs) of the murine MAB into the variable light (V_L) and the variable heavy (V_H) frameworks of a human MAB (Fig. 1.2) (35).

1.3.2 Humanized Monoclonal Antibodies

1.3.2.1 CDR Grafting X-ray crystallographic studies have shown that the contact of antibodies with antigen is through amino acid residues within the complementarity-determining regions (36). Some of the surrounding framework amino acid residues are also involved in interactions with the cognate antigen (36, 37). It is crucial to maintain the CDRs as well as the interactions of the CDRs with each other and the rest of the variable domains if the binding specificity of the MAB is to be preserved. The proper configuration, or conformation, of the binding site requires retention of crucial framework residues, which include those involved in V_H and V_L associations and those that affect the overall domain and combining site structure (36). The necessary framework residues can be identified through high-resolution X-ray crystallographic studies; otherwise, molecular modeling based on the structure of related molecules or the ligand binding properties of site-specific mutants can facilitate identification of required amino acids for correct conformational positioning of CDRs for antigen binding. It is estimated that chimeric antibodies contain ~30% murine sequences; CDR grafting would reduce the nonhuman content to 5–10% (38). Selecting the appropriate human acceptor template for the CDRs is another crucial element for the successful humanization of a murine MAB. The strategy is usually to choose a human template with the greatest sequence homology to the murine MAB being grafted (39). The polymerase chain reaction (PCR) technology has enabled investigators to graft the entirety of CDRs along with the necessary framework residues from a murine MAB into the human frameworks of human Igs (40).

Humanized (hu) MABs have progressed through evaluation in animal models and into clinical trials. Trastuzumab (Herceptin[®], Genentech) that targets HER2 was the first humanized MAB to gain FDA approval (1998) for the treatment of HER2-positive metastatic breast cancer. Three other humanized MABs have since been approved for

the treatment of cancer patients. Two of these, bevacizumab (Avastin, Genentech) and alemtuzumab (Campath-1H, Berlex), are administered as naked MABs and one, Mylotarg (gemtuzumab ozogamicin, Wyeth), is conjugated with the toxin calicheamicin. The naming of drugs is a consensus between the United States Adopted Names system, the inventor/discoverer of the drug, and the FDA. The American Medical Association established the guidelines for assigning generic names of MAB drugs. The foundation to the designation is the suffix "MAB" for monoclonal antibody. Letters, or infixes, before the suffix denote the source, that is, o for mouse, xi for chimeric, zu for humanized, and u for human.

The transition to humanized MABs proved that empirical evaluation of each MAB was required. CAMPATH-1H, an anti-human CD52 MAB, was found to have a lower affinity than the original rat MAB (41). This was remedied when two amino acids in the V_H framework were mutated back to the original rat MAB sequence. In general, preclinical studies have demonstrated that the CDR-grafted MABs retain the ability to react with their tumor antigen. In some instances, the huMABs have had higher affinities than the original murine MAB. HuM195, an anti-CD33 MAB, was found to have a 3–8.6-fold increase in affinity and avidity (42). Other huMABs, that is, MN-14, an anti-CEA MAB, also proved to have improved tumor targeting over the murine MAB (43). In contrast, the CDR grafting of other MABs has yielded Ig molecules with decreased antigen affinity. For example, huCC49 has been found to have a two- to threefold lower relative affinity compared to the murine CC49 MAB (39).

Perhaps more interesting is the plasma pharmacokinetic data collected from clinical trials with some of the huMABs. In general, one would anticipate that a huMAB injected into patients would have a longer residence time in the blood than a xenogeneic muMAB. This was in fact true for some huMABs. The plasma half-life of huBrE-3, a MAB that targets breast epithelial mucin, was twofold greater than that for the murine BrE-3, 114.2 ± 39.2 and 56 ± 25.4 h, respectively (44). This prolonged retention of the radioimmunoconjugate in the blood may result in increased myelotoxicity. However, if the huMAB has reduced immunogenicity, then multiple cycles of radioimmunoconjugate at lower radiation doses (dose fractionation) would be possible and still result in effective RIT. On the other hand, the plasma pharmacokinetics of two other huMABs (MN-14 and M195) proved to be similar to their parental murine forms (43, 45). This latter phenomenon may be reflective of the MAB interacting with antigen and/or tumor cells present in the blood.

As mentioned previously, huMABs possess a murine sequence content of 5–10% and this amount of xenogenic sequence has proven to be sufficiently immunogenic in patients to elicit humoral responses. The huMABs of anti-TAC and anti-CD18 were evaluated in subhuman primates and found to be immunogenic with anti-idiotypic antibody responses detected (46, 47). Humanized anti-TNF α , when administered at doses of 1, 2, 5, and 10 mg/kg, elicited antibody (IgM) responses in normal human volunteers (48). Antibody responses have also been detected in patients receiving weekly 2–4 mg/kg (i.v.) of trastuzumab (49). In general, the protein amounts of radiolabeled MABs that are injected into patients are lower; the immune responses directed against each of these huMABs may not be relevant to the use of radiolabeled MABs. No evidence of a human anti-human antibody (HAHA) response in patients

receiving huJ591, radiolabeled with ^{131}I , ^{90}Y , or ^{177}Lu , has been detected nor has a response been detected in patients receiving as many as three injections of ^{131}I -huMN-14 (45, 50, 51).

Studies have been conducted to characterize the immune response against two MABs in greater detail. Schneider et al. identified specific CDRs in the huMAB anti-Tac that were recognized by antibodies in the sera of cynomolgus monkeys that had received these antibodies (46). The majority of the antibody response was found to be directed against the heavy-chain CDRs 1 and 2 as well as the light-chain CDR3 of the humanized anti-Tac. No detectable response was directed solely against any one CDR or to the modified framework of the human variable regions. A similar study was performed using the serum of a patient who had received ^{177}Lu -labeled muMAB CC49 for RIT (52). In this particular study, the patient's antibody response was determined to be directed toward the heavy-chain CDR2 and the light-chain CDRs 1 and 3 (53). It was also found that these same CDRs were required for antigen binding. The information from such studies led to the development of huMAB using SDR (specificity-determining residue) and abbreviated CDR grafting, with the objective of creating a minimally immunogenic Ig molecule that retained optimal antigen binding and affinity.

1.3.2.2 SDR Grafting The specificity-determining residues comprise only 20–33% of the CDR residues; therefore, the CDRs could be humanized by up to 80% when only the SDRs are grafted (54). The process requires identification of SDR and non-SDR residues within the CDR. When a crystal structure of the antibody–antigen complex is available, SDR/non-SDR residues are readily identified. Lacking the crystal structure, the indispensability of SDR residues can be tested through genetic engineering. Based on known antibody–antigen complexes, it appears that there is little variation in the regions that contain SDRs; antibodies with unknown structures will likely have SDR residues in the same positions. Therefore, only a few variants are required to identify those SDR residues that are required for antigen binding and the non-SDRs can then be replaced with corresponding human residues (54). The muMAB COL-1, which reacts with carcinoembryonic antigen (CEA), was humanized by SDR grafting while huCC49 was subjected to further refinement (14, 55). Variants of both MABs were generated using a baculovirus expression system and tested *in vitro* for antigen binding. One variant of HuCC49 exhibited superior binding and tumor targeting properties compared to the original huCC49. As with the grafting of whole CDRs, it is crucial in SDR grafting that an appropriate human framework is chosen as well as retaining the framework residues that are needed for maintaining the conformation of the antigen binding site. The evaluation of such Ig molecules in clinical trials will determine if the objective of minimizing immunogenicity has been achieved. The affinities of the CDR- or SDR-grafted MABs can be further manipulated with methods such as *in vitro* affinity maturation using phage display techniques (56).

1.3.2.3 Abbreviated CDR Grafting To further reduce the number of murine residues of the huMAB, grafting of only the SDRs into the human Ig framework, coined as “abbreviated” CDR grafting, has been proposed (54). Engineering huCOL-1 in this

fashion resulted in a 2.7-fold decrease in affinity compared to CDR-grafted huCOL-1 and a 4.3–5-fold lower affinity compared to muCOL-1 (57). Unfortunately, these humanized forms were not evaluated *in vivo* for tumor targeting, but the trend in decreasing affinity provides an argument for retaining residues from the murine framework to maintain the binding site conformation of the MAb.

One fact is clear, the insertion of mouse sequences into human sequences and the further replacement of sequences in the Ig to alter properties and reduce immunogenicity of the MAb is laborious, requiring remodeling and engineering MAb by MAb. After all of these manipulations, mouse sequences remain and even though each step has reduced the immunogenicity, the molecules still elicit an antibody response in patients.

1.3.3 Human Monoclonal Antibodies

Human MAbs against tumor-associated antigens are believed to be the ideal agent for clinical applications. One of the main obstacles to administering a xenogeneic protein, immunogenicity, would be absent, or minimal, if a syngeneic antibody was available. The biological characteristics (metabolism and pharmacokinetics) (58) would, however, differ appreciably from muMAbs. Human MAbs have been generated that are reactive with antigens present in human tumors by fusing lymphocytes (myeloma cells) from cancer patients, thus creating human–human hybridomas. However, very few have demonstrated the necessary specificity or affinity to merit their use in clinical trials (59, 60). Inherent human tolerance to human antigens along with the reality that human subjects will not undergo the immunization regimen required to generate antibodies has understandably limited the possibilities. Recombinant DNA technology has hence provided the tools to create completely human MAbs. In the early 1980s, the race began to create a transgenic mouse for human Ig that possessed the heavy- and light-chain repertoires that would be capable of generating a secondary immune response that would result in high-affinity antibodies. Strategies taken to accomplish this utilized homologous recombination in mouse embryonic cells to disrupt the endogenous heavy- and light-chain genes. Construction and introduction of human unrearranged gene segment sequences is where strategies differ. One method used fusions of yeast protoplasts to deliver yeast artificial chromosome (YAC)-based minilocus transgenes into mouse embryonic cells (61). A second method used pronuclear microinjection of reconstructed minilocus transgenes into the mouse cell (62). The numbers of heavy-chain variable (V), diversity (D), and joining (J) segments varied in each of these transgene reconstructions and were not the whole repertoire. However, each could be shown to undergo VDJ joining and class switching in the transgenic mice. In both studies reported, the mouse heavy-chain genes were inactivated, the light-chain genes were not, and expression of a functional mouse light chain was observed. Further analysis determined that the resulting subpopulation of B cells did not interfere with the isolation of hybridoma cell lines that secreted fully human MAbs that were reactive with the immunizing antigen. Subsequently, transgenic mice have been created that express complete human heavy- and light-chain repertoires with high-affinity MAb isolated (63, 64).

There is also the *in vitro* approach to generate human MAbs using phage display. Methods were developed for cloning expressed Ig variable region cDNA repertoires to create phage display libraries of antibody variable fragments. Sequences can be selected based on the desired properties and then enriched (65). The libraries are restricted to the donor's exposure to antigen, which dictates whether early or mature B-cell response Igs are present for selection. The technology has been further refined since the first description of generating antibody variable domains with affinity maturation (66).

The first fully human MAb that gained FDA approval in 2002 was created using the phage display platform; adalimumab, an anti-TNF α antibody, was approved for the treatment of inflammatory diseases (67). Panitumumab (Amgen and Abgenix), approved in 2006 for the treatment of patients with EGFR-expressing metastatic colorectal cancer, is the first commercially available human MAb generated using transgenic mice (68, 69). The human MAbs have been well tolerated and to date appear to be less immunogenic than the chimeric MAbs (69). High-affinity human MAbs have been generated with specificities for numerous antigens that include cytokines, growth factors, CD antigens, and nuclear factor receptors using both phage display and transgenic technologies (67). A survey of the literature suggests that the latter approach though may be the favored route to obtaining human MAbs. In a recent report tabulating selected human MAbs that are in clinical development, 45 are from transgenic mice while 16 are from phage display libraries (67). Thirty-five of these human MAbs were developed as cancer therapeutics with 28 derived from transgenic mice. The favoring of the transgenic mouse platform most likely is a reflection of the processes involved in moving from discovery to the clinical setting. In general, the MAbs that are initially identified when generated from a transgenic mouse will go into production and development without the need for further manipulation. In contrast, it appears that the phage display-generated MAbs have consistently required additional tweaking such as affinity maturation.

1.4 NANOBODIES

Nanobodies are the smallest antigen binding regions or fragments of naturally occurring heavy-chain antibodies (HCAs). Lacking a light chain, these fully functional HCAs were identified as part of the humoral response in camels, dromedaries, and llamas (Camelidae) (70). HCAs have also been identified in wobbegong and nurse shark (71). The structure of the HCAs consists of a single variable domain (VHH), a hinge region, and two constant domains, C_H2 and C_H3 (Fig. 1.3). The VHH region contains three CDRs for antigen binding. The HCAs lack the C_H1 domain, which is actually contained in the genome, but is spliced out during mRNA processing. This absence would explain the lack of light chain since it is the C_H1 domain that interacts with the C_L domain of the light chain. The CDRs of HCAs appear to be structurally larger, those from the dromedary contain 16–18 amino acids (a.a.), compared to human (12 a.a.) or mouse (~9 a.a.) CDRs. This structural difference might serve as a means of providing a larger repertoire to the organism

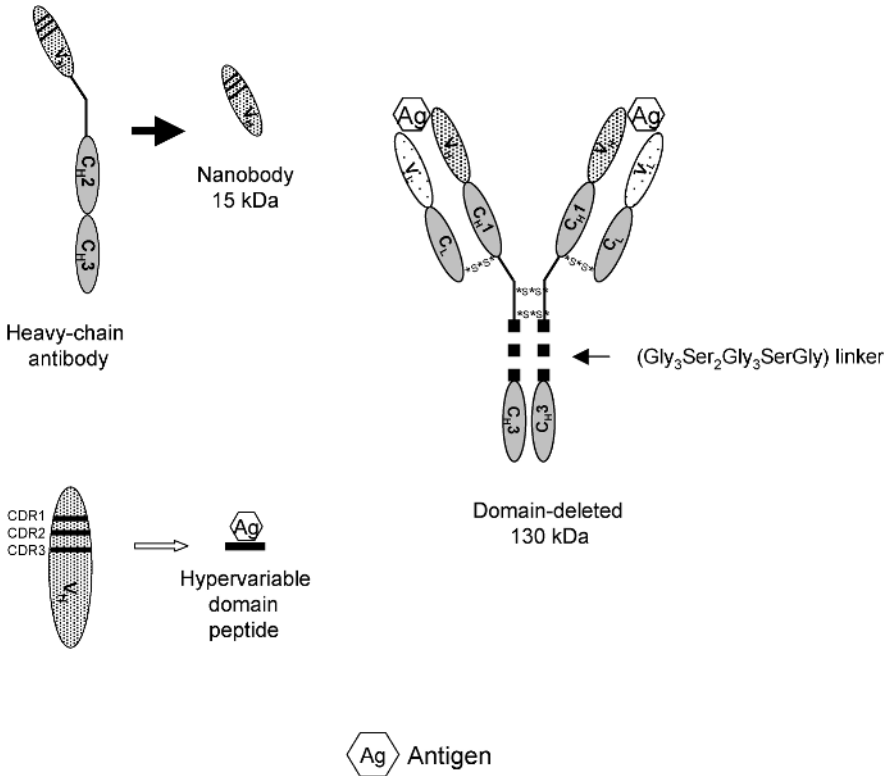


FIGURE 1.3 Illustration of a heavy-chain antibody, nanobody, domain-deleted MAb, and a hypervariable domain peptide.

since the V_L region and three CDRs are missing. CDR3 appears to be more exposed and the antigen binding site of the V_HH also has protruding loops. This has the affect of increasing the surface of the HCAb paratope, making it as large as conventional antibodies.

The single domain of nanobodies (Fig. 1.3) simplifies the cloning, expression, and selection of antigen-specific molecules. Only one set of primers is needed and the HCAb has undergone affinity maturation *in vivo*; therefore, the library is relatively small (10⁶–10⁷ nanobody genes) from which high-affinity nanobodies are isolated (72). The nanobodies are soluble, nonaggregating proteins with an M_r of 15 kDa and can easily be produced in bacterial or eukaryotic systems. High-level nanobody production has been noted in a variety of expression systems (73). Nanobodies have also been shown to have high thermal and conformational stability. The melting points of the nanobodies range from 60 to 78 °C; following incubations at 90 °C, they have regained antigen binding/specificity (71). With such properties, nanobodies may prove to have a long shelf-life and may be manipulated under conditions not acceptable for other antibody forms such as radiolabeling at higher temperatures to obtain higher labeling efficiencies.

Radiolabeled nanobodies have been shown to efficiently target tumor xenografts in mice by microSPECT/CT and biodistribution studies. For the former, images of tumor xenografts were obtained 1 h after i.v. injection of anti-EGFR nanobodies labeled with ^{99m}Tc (74). For the latter, Balb/c mice bearing syngeneic tumors were injected i.v. with ^{125}I -labeled nanobodies that react with lysozyme. Tumor targeting was demonstrated at 2 and 8 h post-injection. More importantly, this study was conducted in immunocompetent mice; no antibody or T-cell responses were detected against the nanobody, suggesting that the nanobodies may not be immunogenic or their immunogenicity is very low, at least in this host (75). The single domain nature of nanobodies along with their physical properties makes them particularly interesting and appealing as a delivery vehicle for radionuclides or any other desired payload.

1.5 DOMAIN-DELETED MONOCLONAL ANTIBODIES

The recent advances in molecular cloning that led to the CDR grafting of MAbs have also led to modifying the domains of MAbs to alter their biological properties, that is, pharmacokinetics, with the objective of optimizing their therapeutic potential. Gillies and Wesolowski were the first to construct a $\text{F}(\text{ab}')_2$ fragment using genetic engineering techniques (76). They were unable to generate a bivalent molecule, nor were the resulting molecules reactive with antigen. In the pursuit of determining what portions of the Ig molecule were required for antigen binding, a construct with a $\text{C}_{\text{H}2}$ domain deletion was generated (Fig. 1.3) (77). This new MAb form, in this case a construct from chimeric MAb 14.18, which recognizes the ganglioside GD2, demonstrated a significantly faster elimination from the plasma compared to the intact and aglycosylated form of the same MAb. The pharmacokinetics was found to be similar to human IgG $\text{F}(\text{ab}')_2$ fragments. Maximal tumor targeting with radiolabeled $\text{ch}18.14\Delta\text{C}_{\text{H}2}$ occurred at 12–16 h versus 96 h postinjection for the intact $\text{ch}18.14$. In addition, the domain-deleted variant did not exhibit the renal uptake of radioactivity that is usually associated with radiolabeled $\text{F}(\text{ab}')_2$ fragments (78). A similar $\text{C}_{\text{H}2}$ domain-deleted chimeric antibody of MAb B72.3 was reported by Slavin-Chiorini et al. (79). The $\text{ch}B72.3\Delta\text{C}_{\text{H}2}$ differed from the $\text{ch}18.14\Delta\text{C}_{\text{H}2}$ in that a 10-amino acid linker (gly₃-ser₂-gly₃-ser-gly) was inserted in place of the deleted $\text{C}_{\text{H}2}$ domain, which provided stability to the molecule. Domain-deleted mutants have subsequently been produced of chimeric and CDR-grafted humanized forms of MAb CC49 that have been analyzed in preclinical *in vitro* and *in vivo* studies (80, 81). A $\text{C}_{\text{H}1}$ domain-deleted mutant of $\text{ch}CC49$ was also produced and was compared to $\text{ch}CC49$ and the $\text{ch}CC49\Delta\text{C}_{\text{H}2}$ Ig forms (81). The $\text{ch}CC49\Delta\text{C}_{\text{H}1}$ exhibited pharmacokinetics and tumor localization that were similar to those of the intact $\text{ch}CC49$. In contrast, the pharmacokinetics of the $\text{ch}CC49\Delta\text{C}_{\text{H}2}$ was significantly faster in nontumor bearing athymic mice and rhesus monkeys than $\text{ch}CC49$. Tumor targeting was also more efficient and occurred within an earlier time frame than that of $\text{ch}CC49$. When labeled with a radiometal, that is, ^{177}Lu , the pharmacokinetics exhibited a profile similar to ^{131}I - $\text{ch}CC49\Delta\text{C}_{\text{H}2}$. The domain-deleted $\text{hu}CC49$ has demonstrated these same desirable characteristics (80). The $\text{hu}CC49\Delta\text{C}_{\text{H}2}$ has shown efficacy in animal models

for the treatment of peritoneal tumor deposits and subcutaneous tumors when radiolabeled with ^{177}Lu and ^{213}Bi , respectively (82, 83).

Two clinical trials with huCC49 $\Delta\text{C}_{\text{H}2}$ have been conducted (84, 85). The first was a small pilot study of four colorectal cancer patients receiving 10 mCi (370 MBq) of ^{131}I -huCC49 $\Delta\text{C}_{\text{H}2}$ (84). Pharmacokinetics, biodistribution, dosimetry, and immune responses were evaluated. Targeting of metastatic disease was observed in all patients with no toxicities reported. The mean plasma elimination half-life was 20 ± 3 h with a mean residence time of 29 ± 2 h; this was a faster elimination rate than murine CC49. One of the patients appeared to develop a detectable antibody response at 6 weeks. The second trial enrolled 21 patients with recurrent and metastatic colorectal cancer (85). In this trial in which patients were administered 2 mCi (74 MBq) of ^{125}I -huCC49 $\Delta\text{C}_{\text{H}2}$, the pharmacokinetics was found to be similar to murine CC49, tumors were detectable, and no antibody response to the injected huCC49 $\Delta\text{C}_{\text{H}2}$ was detected. Overall, the investigators performing the trials reported that the huCC49 $\Delta\text{C}_{\text{H}2}$ was well tolerated.

Production of chCC49 $\Delta\text{C}_{\text{H}2}$, huCC49 $\Delta\text{C}_{\text{H}2}$, and chB72.3 $\Delta\text{C}_{\text{H}2}$ was found to result in what initially appeared to be impurities by SDS-polyacrylamide gel electrophoresis. The impurities were subsequently identified as isoforms of the domain-deleted molecules. Form A was proposed to contain the appropriate interchain disulfide between the two heavy chains. Form B was thought to be a result of the heavy chains associating through noncovalent interactions of the $\text{C}_{\text{H}3}$ domains. Instead of the disulfides forming interchain bonds, form B contained intrachain bonds. To favor production of form A with the interchain disulfide bonds, investigators at Biogen Idec modified the hinge region linker sequence to stabilize the hinge region and thus favor the correct disulfide bond formation (86). Insertion of a cysteine-rich 15-amino acid IgG₃ hinge motif along with an additional alanine and proline resulted in a product that was 98% form A isoform, with little or no form B detected. This alteration of the hinge region, unfortunately, resulted in a 1.4-fold decrease in the affinity of the huCC49 $\Delta\text{C}_{\text{H}2}$ (86).

1.6 HYPERVARIABLE DOMAIN REGION PEPTIDES

It is the CDRs in the variable domains that interact with the antigen epitope (36). As previously mentioned, this interaction depends on the tertiary structure of the antigen combining site. However, in some instances, the CDR sequence that interacts with the antigen may be linear. As a result, hypervariable (HV) domain region peptides, or molecular recognition units (MRUs), may be identified and synthesized that can target and bind to tumor-associated antigens (Fig. 1.3). A peptide, designated $\alpha\text{M}2$, was synthesized based on the heavy-chain CDR3 and some framework residues of the anti-MUC-1 antibody, ASM2 (87). Analysis of the $\alpha\text{M}2$ peptide determined that it adopted the β -strand conformation of the antigen binding structure of the intact MAb. Radiolabeled peptide was able to bind antigen, albeit at a lower affinity. Studies with the $\alpha\text{M}2$ peptide progressed to a pilot clinical study. Twenty-six women with primary, recurrent, or metastatic breast cancer were injected with $^{99\text{m}}\text{Tc}$ -labeled $\alpha\text{M}2$ (87).

Optimal radioimmunodetection occurred by 3 h postinjection and 77% of known lesions were visualized.

Reducing the antigen–antibody interaction to a single CDR may increase the potential for cross-reactivity with other antigens. Furthermore, the use of HV peptides is limited to those antibody–antigen interactions that do not rely on spatial conformations. Either of these obstacles, however, may not be insurmountable. Through molecular modeling and other sophisticated techniques, peptides may be designed with improved binding properties. Higher affinity binding HV peptides have been obtained by either dimerizing or constraining the conformation of the HV peptide by introducing cysteine residues that result in looping of the peptide and restricting the conformations it could assume as a linear peptide (88). It is also conceivable that HV peptides will be designed and synthesized with chelates or additional amino acids to facilitate labeling with radionuclides and/or to increase the specific activity of the radioimmunoconjugate for RIT procedures. The rapid pharmacokinetics in conjunction with the ease of synthesizing and producing peptides are desirable characteristics for radiopharmaceutical development.

1.7 FV FRAGMENTS

In 1988, single variable domains of a mouse Ig were expressed in *Escherichia coli* and shown to be functional (89, 90). Again, where enzymatic methods were limited and greatly variable in reproducibility, recombinant technology has greatly facilitated the generation and production of this antibody form. Fv fragments (Fig. 1.4) consist of the V_L and V_H domains of the antibody molecule. The associations between the domains are weak noncovalent interactions due to the lack of the C_{H1} and C_L domains (91–93). In many cases the V_L – V_H associations were found to be reproducible and resulted in a functional binding site (92, 94). Unfortunately, the Fv fragments dissociated at low protein concentrations and were found to be unstable at physiological temperatures. The strategies taken to obtain stable Fv fragments were (i) chemical cross-linking, (ii) engineering of disulfide bonds into the molecule, or (iii) the insertion of a peptide linker between the V_L and V_H domains (Fig. 1.4). The employment of the peptide linker has been the most favored strategy and the resulting Ig form has been designated as scFv (single-chain Fv). The scFv is constructed by connecting the V_L and V_H genes with an oligonucleotide that encodes 15–25 amino acids and is expressed as a single polypeptide chain (89, 95). The variable domains can be assembled in either order (V_H – V_L or V_L – V_H) with examples in the literature of one orientation proving superior to the other (96, 97). The most common linker is $(Gly_4-Ser)_3$; linkers of 18-amino acid residues, or more, have been found to favor folding of the scFv resulting in a monomer form (98).

The scFv form has demonstrated several advantages over intact Ig MAbs, $F(ab')_2$, and Fab' fragments. The pharmacokinetics of elimination of the scFv and clearance from normal tissues is appreciably faster (22, 99). In therapeutic applications, this would translate to a reduction in radiation exposure to normal tissues. It has also been shown that scFvs penetrate tumor tissue more rapidly, farther, and with a greater

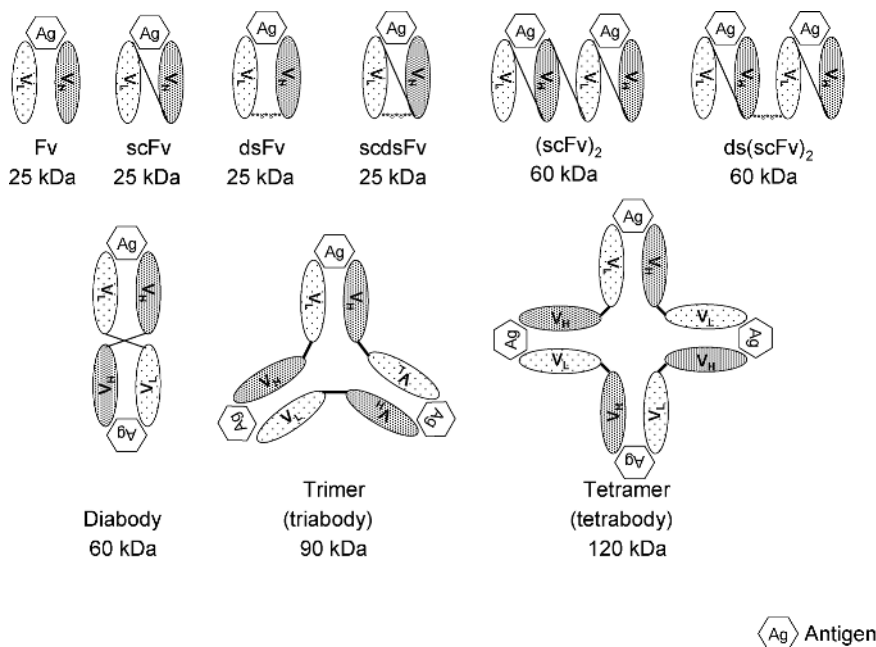


FIGURE 1.4 Schematic diagram of the various Fv forms.

degree of homogeneity (21). With these properties, scFvs have the potential of delivering a radiation dose more homogeneously throughout a tumor lesion (100). However, the low %ID/g may not permit the delivery of an adequate therapeutic dose of radioactivity if it is not matched with a radionuclide of an appropriate half-life (101).

Since scFv molecules have such rapid pharmacokinetics, the overall amount that accumulates in the tumor is low. The tumor uptake of two scFvs, both labeled with ^{125}I and evaluated in the same tumor model, ranged from 0.3 to 3.4%ID/g at 24 h postinjection with tumor-to-blood ratios ranging from 3.8 to 26.5 (22, 102). The tumor %ID/g at 24 h for the scFv of CC49 was 12.5-fold lower than that obtained with the intact murine CC49 MAb (22). Due to the low percentage of the radioimmunoconjugates in the blood, the scFv was actually a more attractive candidate for RIT especially when labeled with a short-lived radionuclide such as one of the α -emitters that are very potent even at low amounts of radioactivity delivered to tumors (100).

In general, the scFv has a diminished affinity, which is related to the loss of the second antigen binding site (bivalency) that would stabilize the antigen-antibody interaction (22). In one instance, an scFv was reported to have an affinity constant comparable to the parental IgG (99). Adams et al. (103) have been able to enhance the affinity of the scFv of C6.5 (which recognizes HER2/*neu*) through site-directed mutagenesis. Using a phage display library, C6.5 scFv mutants were isolated that varied 320-fold in their affinity compared to the nonmutated C6.5 scFv. The mutant with the highest affinity differed in only three amino acids in the V_L CDR3. This high-affinity mutant scFv showed a twofold increase in the ability to target tumor.

The mutant also demonstrated an improvement in the radiolocalization indices (tumor-to-normal organ ratio). More elegant studies by the same group have evaluated the effect of affinity on scFv tumor targeting, intratumoral diffusion, and tumor retention in greater detail (104). Variants of an anti-HER2/*neu* scFv were produced with affinities from 10^{-7} to 10^{-11} M. Biodistribution studies comparing these scFvs radiolabeled with ^{125}I revealed that tumor uptake/retention did not significantly increase beyond an affinity of 10^{-9} M and the differences in the pharmacokinetics of the scFvs were not a function of renal clearance. Immunohistochemical analysis of tumor xenografts following injection of the scFv affinity variants indicated that the scFvs with the lower affinity distributed diffusely throughout the tumor. Meanwhile, the scFvs with the higher affinities were localized primarily to the perivascular regions of the tumors. The implication is that antibody-based molecules with high affinities are restricted in their ability to penetrate tumors, which is yet another consideration in designing a targeting agent.

The ability of scFv to target tumor efficiently and to clear from normal tissues has been investigated in the clinical setting. Single-photon emission computed tomography (SPECT) and whole-body planar imaging were performed with CC49 scFv, radiolabeled with ^{123}I (105). Tumors were visualized; uptake of the radioimmunoconjugate by tumor tissue was determined directly from biopsy samples. The scFv was also determined to have a biphasic clearance with a distribution half-life ($T_{1/2\alpha}$) of 30 min and elimination half-life ($T_{1/2\beta}$) of 10.5 h. The patients did not receive any treatment to inhibit renal sequestration of the radiolabeled scFv; thus, significant uptake was evident in the kidneys. Similar results were also reported with an anti-CEA scFv radiolabeled with ^{123}I (106). More recently, promising results were reported for an anti-CEA scFv (MFE-23) for application in radioimmunoguided surgery (107). In this particular study, the $T_{1/2\beta}$ of the MFE-23 scFv was twofold greater than that reported previously.

An alternative to the peptide linker for stabilizing the orientation of the V_H and V_L domains has been the use of disulfide bridging introduced through cysteine residues in the sFv. This strategy has proven quite effective; disulfide sFvs (dsFvs) have been produced with reactivity against the IL-2 receptor, LYM-1, Lewis Y-related carbohydrate, CD19, and p185^{HER2} (108–112). As with the sFvs, the dsFvs have shown good tumor targeting, with rapid pharmacokinetics and excellent tumor-to-normal tissue ratios.

The combination of the peptide linker with disulfide bridging has also been explored as a means of providing stability and proper binding site configuration. The purification yield of this form, a single-chain dsFv (scdsFv), is appreciably better than that of the scFv form, with less aggregation occurring in the final product (113). In addition, the *in vitro* and *in vivo* properties of the scdsFv have proven to be equivalent to the scFv form (113, 114).

1.7.1 Multimeric Fv Forms

A variety of multimeric Fv forms have been created and assessed with the goal of improving the affinity of Fvs with desired pharmacokinetic properties. These

multimeric forms include Fv dimers (diabodies), Fv trimers (triabodies), Fv tetramers, and minibodies. In addition, multimeric Fvs have been created with mono- and bispecificity. Diabodies (55 kDa) are noncovalent dimers of scFv fragments that are formed using short peptide linkers (3–12 amino acids) that promote cross-pairing or association of the V_H and V_L domains of two polypeptides (Fig 1.4) (115, 116). A scFv dimer of MAb T84.66, labeled with ^{125}I , was reported to have a three- to fivefold greater uptake in tumor than its scFv monomer counterpart with reduced radioactivity uptake observed in the kidneys (102). When labeled with the radiometal, ^{111}In , the T84.66 diabody again demonstrated good tumor targeting; however, renal and hepatic accumulation of radioactivity remained a problem (117). Diabodies have also been generated for the MAb CC49 scFv and the anti-HER2/*neu* scFv (C6.5) that were also found to have improved tumor targeting over their scFv monomer form (22, 118, 119). The C6.5 diabody was reported to have an increase in affinity of 40-fold over the C6.5 scFv. In contrast to the aforementioned scFv dimers, a diabody of the anti-MUC1 C595 MAb, created by replacing the $(\text{Gly}_4\text{-Ser})_3$ with $(\text{Gly}_6\text{-Ser})_3$, displayed binding reactivity to MUC-1 that was similar to the intact MAb C595 (120). Similar findings were reported for a dimer of the anti-HER2/*neu* scFv that was prepared in a comparable manner (118).

The use of diabodies for targeted radiation therapy has been pursued using the α -emitting radionuclides, ^{213}Bi and ^{211}At (121, 122). The rapid pharmacokinetics of a diabody presents itself as a good match with the half-lives of these radionuclides (^{213}Bi at 45.6 min and ^{211}At at 7.2 h). In a therapy study treating subcutaneous (s.c.) ovarian carcinoma xenografts with the ^{213}Bi -C6.5 diabody, acceptable toxicity occurred at the lowest dose administered (121). To minimize renal exposure to the ^{213}Bi , mice were pretreated with D-lysine. Unfortunately, the therapeutic effect was found to be nonspecific, leading the investigators to conclude that the half-life of the ^{213}Bi was too short to be effectively paired with a systemically administered diabody. A subsequent study pairing ^{211}At ($t_{1/2} = 7.2$ h) and the C6.5 diabody proved more successful in the therapy of HER2-positive breast cancer tumor xenografts (122). A single i.v. injection of ^{211}At -C6.5 diabody resulted in durable complete responses in 60% of the mice; the remaining mice experienced a significant delay in tumor growth. The C6.5 diabody has also been shown to be an effective vehicle for targeting the β -emitter, ^{90}Y (123). Growth inhibition of breast and ovarian cancer xenografts in mice was reported; the maximum tolerated dose appeared dependent on the tumor model. Renal toxicity of the ^{90}Y -C6.5 was evaluated in nontumor bearing mice with mixed results. One mouse showed no overt signs of renal damage, another demonstrated early-stage renal disease, while a third had severe kidney damage. Renal toxicity was also evaluated in the ^{211}At study. After 1 year, histopathologic examination of the kidneys revealed that two of the three mice exhibited regions of fibrosis amidst healthy tissue (122). This renal damage was modest compared to that observed in the mice that received the ^{90}Y -C6.5, providing an argument for the pursuit of the halogen-based radioisotopes for therapeutic applications with diabodies as the targeting vector.

Noncovalent trimers (triabodies) and tetramers (tetrabodies) have also been produced and evaluated. Initial studies with scFvs had made it apparent that several

factors such as the length of linker sequences connecting the V_H and V_L domains, the linker composition, as well as concentration of the molecules influence the formation of multimeric Fv molecules (97, 116, 124). Several multimers of the anti-Lewis Y antigen MAb, HuS193, were created by directly ligating the V_H and V_L domains by either inserting one or two amino acid residues or removing one or two amino acids (97). The addition of residues favored the formation of dimers while the direct linkage of the domains, or the removal of amino acids, led to the trimeric and tetrameric forms. The stability of the multimers was directly related to the apparent affinity of the domains for each other. This study also illustrates the difficulty in maintaining a homogeneous product. Over a 2-week period, the investigators found that a solution of a given multimer would contain other sizes of multimers suggesting the formation of multimers is a dynamic process. The engineering of “knobs into holes”, that is, the introduction of amphipathic helices or leucine zipper motifs into the scFv molecule, is one of the measures being taken to enhance the formation of the noncovalent multimeric forms (125–127).

An alternative to the noncovalent multimeric scFv forms are those that are covalently associated. Difficulties of diabodies arise from their inherent compactness and inflexibility. The two binding sites in this Ig form are in an opposing orientation to each other, which may restrict interactions with antigen at both combining sites. The introduction of a peptide linker between the two scFv chains, tethering the V_H domain of one chain with the V_L domain of the other chain, not only lends stability to the molecule but also maintains the binding sites in an appropriate configuration for interacting with antigen (Fig. 1.4). Recently, Beresford et al. (119) compared two dimeric scFv forms (covalent and noncovalent) of MAb CC49. The covalent form was found to target tumor and had pharmacokinetics similar to the noncovalent form. The two forms differed in their tumor-to-normal tissue ratios, with the covalent form yielding superior ratios. This dimeric CC49 scFv utilized a helical linker, consisting of 25 amino acids, connecting the V_H and V_L domains of each peptide chain as well as the two chains (128). In the same study, the investigators also modified the charge of the scFv and evaluated the effect on renal retention of the scFv. Negatively charged amino acids were added to the carboxyl terminus of the CC49 V_H by including oligonucleotide sequences in a polymerase chain reaction amplification. Interestingly, decreasing the isoelectric point of the scFv molecule from pH 8.1 to pH 5.1 did not significantly affect the accretion of the scFv in the kidney; it is believed that cationic amino acids promote renal uptake.

Studies have progressed with the dimeric CC49 scFv with the creation and evaluation of a tetravalent molecule designated $[\text{sc}(\text{Fv})_2]_2$ (Fig. 1.4) (129, 130). This molecule consists of CC49 scFv dimers that are noncovalently associated through interactions between opposing V_L and V_H domains of each dimer. When compared to the CC49 scFv dimer and the original CC49 MAb, all radioiodinated, the tetravalent molecule was comparable to the IgG in its affinity as well as in overall tumor uptake. Where the CC49 $[\text{sc}(\text{Fv})_2]_2$ differed was in its clearance from the blood. The tetravalent molecule had a residence time that was twofold longer than the dimer, but was twofold shorter than the IgG. The same pharmacokinetic behavior was observed when the CC49 $[\text{sc}(\text{Fv})_2]_2$ was labeled with ^{177}Lu . More surprising was the

fact that high renal uptake of the radioimmunoconjugates occurred that could not be abrogated with pretreatment of the mice with D-lysine (131). This *in vivo* behavior is inconsistent with a molecule with a molecular weight of ~ 120 kDa, since the threshold for renal filtration of proteins is < 50 kDa. In theory, the tetravalent form should not be subjected to first-pass renal clearance. The renal uptake and faster pharmacokinetics of the tetravalent molecule may be a result of its dissociation into its two dimer components. In a subsequent study, both the divalent and the tetravalent molecules were found to form higher molecular weight species in the serum but with time, lower molecular weight species appeared, suggesting degradation, thus providing an explanation for the results of the earlier study (130).

The introduction of cysteine residues in the C-terminus of the V_H and V_L domains has also been employed to create multimeric forms via disulfide bond formation. A divalent scFv of the anti-HER2/*neu* MAb 741F8 was prepared in this manner by Adams et al. (132). Compared to the monomer scFv, an improvement in tumor targeting was observed that was attributed to the increased avidity of the divalent 741F8 scFv molecule.

Adams et al. (133) have provided proof that improved tumor uptake is a function of the valency rather than due to a longer retention time in the blood of the larger molecules. Cysteinyll residues (Ser-Gly₄-Cys) were introduced at the COOH-terminal of an anti-HER2/*neu* scFv and an anti-digoxin scFv creating an scFv' of each. Monospecific (scFv')₂ with each specificity and a bispecific (scFv')₂ consisting of anti-HER2/*neu* and anti-digoxin scFv' were constructed and compared *in vivo*. The monomer scFv of each was also included in their comparison. The homodimer of the anti-HER2/*neu* resulted in tumor uptake that was threefold higher than the heterodimer at 24 h postinjection while the blood levels of all three (scFv')₂ molecules were similar.

1.8 MINIBODIES

Another route to provide a multivalent fragment with a molecular weight greater than the 60 kDa molecular cutoff for renal elimination is to reintroduce Ig domains that homodimerize. One such molecule is the minibody that is constructed by ligating the gene encoding the scFv to the human IgG₁ C_{H3} domain. Dimerization of two polypeptide chains occurs spontaneously as a result of interactions between the two C_{H3} domains. The minibody resembles a F(ab')₂ antibody fragment in size ($M_r \sim 80$ kDa for the minibody versus ~ 100 kDa for F(ab')₂) and bivalency. Two forms of this novel engineered Ig have been generated from MAb T84.66, an anti-CEA MAb, and evaluated (134). One, designated LD minibody, contains a two-amino acid peptide between the V_H and C_{H3} domains on each of the chains. The other minibody form, termed Flex minibody, contains the human IgG₁ hinge region and a 10-amino acid peptide linker to the C_{H3} domain (Fig. 1.5). The Flex minibody has the advantage of covalent linkage via the formation of disulfide bonds in the hinge region. *In vitro* analysis of the two T84.66 minibody forms indicated that both molecules maintained binding affinity. The Flex minibody was very slightly better than the LD minibody with affinity constants (K_a) of 2.7×10^9 and 2.0×10^9 M⁻¹, respectively (134). *In vivo*

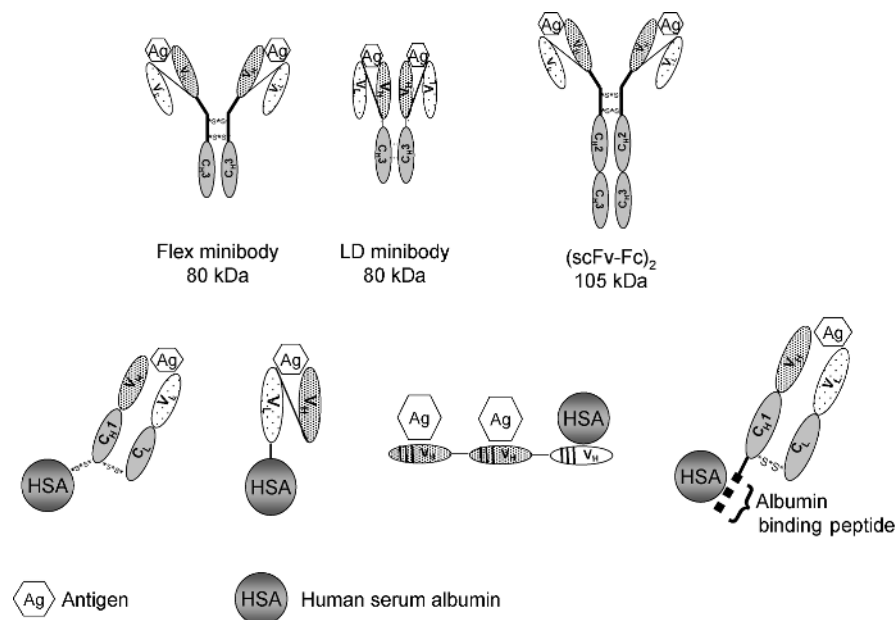


FIGURE 1.5 Schematic representation of different minibody formats and modification strategies.

studies revealed excellent tumor targeting of both molecules, as well as stability in serum. The Flex minibody demonstrated an overall higher %ID/g in the tumor than did the LD minibody and as such was taken forward for further characterization. When labeled with ^{111}In , the minibody maintained good tumor uptake and, in contrast to the diabody, renal uptake was lower. Unfortunately, high hepatic uptake occurs that is comparable to or higher than that observed in the tumor (117). The observed uptake may be antigen driven since a lower percentage of the radioactivity accumulated in the liver in nontumor bearing mice. The hepatic uptake may restrict the use of minibodies to radioiodine labeling or perhaps a short-lived α -emitter such as ^{211}At for therapeutic applications. In fact, the T84.66 minibody has progressed from preclinical studies to a pilot clinical trial labeled with ^{124}I and ^{123}I , respectively (135, 136). In the clinical trial, 10 colorectal patients were injected with ^{123}I -labeled T84.66 minibody and imaged over 2–3 days. The mean serum residence time of the minibody was 29.8 h, 4.3–5.6-fold longer than that observed in the mouse model (117, 134). Tumor imaging was observed in seven patients. The findings of the minibody scans were compared to CT (computed tomography) scans and confirmed by surgery. Three patients had lesions reported as false negative by CT that were detected (positive) by minibody nuclear scans; one false positive by CT was found as a true negative with the minibody scans. Three patients underwent PET imaging, the results of which agreed with the minibody scans. These findings suggest that the minibody has potential for targeted radiotherapy applications.

A minibody has since been engineered with specificity for HER2/neu with the purpose of expanding the repertoire of these molecules (137). The pharmacokinetics

was found to be similar to the T84.66 minibody; however, the tumor uptake was lower, which may simply be due to differences in the animal model and the molecule being targeted.

1.9 SELECTIVE HIGH AFFINITY LIGANDS

Monoclonal antibodies generated against “tumor antigens” have in turn been useful in the identification, isolation, and purification of the antigens themselves. In some instances, identification of a MAb epitope has been reported (138). As indicated previously, the hypervariable domain of the heavy and light chains of several MABs has been sequenced (139). Information such as this has allowed investigators to design and synthesize small molecules that bind to cavities within epitopic regions. These antibody mimics, designated selective high-affinity ligands or SHALs, are attractive targeting vehicles of radionuclides for tumor imaging or radiotherapy (140–143). With the objective of developing a more effective therapeutic for non-Hodgkin’s lymphoma patients, SHALs have been synthesized and tested for efficacy in animal models and reactivity with patient tumor biopsy samples. The first-generation molecules were bidentate, consisting of two ligands linked by polyethylene glycol (PEG) and having a molecular weight <3 kDa (143). In order to improve affinity, a dimer was also synthesized. The SHALs demonstrated selective or specific binding for the target antigen (HLA-DR10) with nM affinities. Unlike the parental MAb (Lym-1), they did not inhibit cell growth or induce the death of lymphoma cells. It was also realized that although the dimeric SHAL was designed to dock into two cavities, that was not the case; it was concluded that the linker was too short to permit bivalent binding. SHALs are readily conjugated with bifunctional chelates such as DOTA and labeled with radiometals efficiently. High radiochemical yields and high specific activities, that is, 2.1–5.3 MBq/μg, can be obtained (141). Several SHALs were compared *in vivo*, and as expected a very rapid clearance from the plasma compartment was observed. Surprisingly, considering the small size of these molecules, low renal uptake was observed, much lower than that reported for scFvs (141). With the feasibility of the SHALs confirmed, the focus of the work with these molecules will be on synthesizing SHALs with higher affinities, optimizing the linkers for dimeric forms and creating multidentate forms using additional SHALs for other antigen cavities (140). The synthetic nature of SHALs should make these molecules attractive to pharmaceutical companies at the level of production and from a regulatory viewpoint. Their rapid clearance from the blood, the ease of radiolabeling, and the high specific activities that can be attained certainly make them attractive candidates for targeted radiotherapy as well as imaging.

1.10 AFFIBODIES

By now it is apparent that evolving techniques in molecular biology have led to targeting agents of ever decreasing size. This section entails describing small

nonantibody affinity ligands (M_r 8.7 kDa) designated affibodies. These molecules are based on a 58-amino acid domain derived from staphylococcal protein A that binds Ig (144). The Z domain is a cysteine-free three-helix bundle that has been used as a platform to generate a number of affibodies (144). The first cancer target for which affibodies were generated and evaluated was HER2 (145). Phage display technology was used to isolate affibody ligands specific for the extracellular domain of HER2 (HER2-ECD). Four rounds of selection resulted in the sequencing of 49 colonies. Analysis of the sequencing indicated that there were actually seven colonies represented, one of which appeared 33 times; the dominance of this sequence is an indicator of the high binding affinity of this particular affibody. Four affibodies were chosen for production, purification, and further characterization. All bound to HER2-ECD (extracellular domain) with affinities in the nanomolar range; one of the two that were radiolabeled with ^{125}I demonstrated binding with HER2-positive cells (145). The small size, stability, and high affinity of affibodies render the molecules attractive candidates for tumor targeting applications. As a monovalent binding agent, the dissociation rate of the affibody from the target molecule was too rapid. Thus, studies with affibodies have progressed with the goal of improving affinity, which has been achieved through the head-to-tail dimerization of two affibodies resulting in a molecule with an M_r of ~ 15.6 kDa (146). The bivalency resulted in a product with an affinity that was improved by ~ 17 -fold, which approximates that of trastuzumab. The *in vivo* potential of the bivalent affibody [$(Z_{\text{HER2:4}})_2$] was demonstrated by biodistribution and imaging studies (147). Radiolabeled with ^{125}I , tumor uptake was observed with minimal uptake in normal organs. Renal uptake was also observed but the values were still within acceptable levels. A second generation of affibodies has been since produced with affinity constants in the picomolar range (148). This was achieved through affinity maturation, a process in which random mutagenesis of select amino acids is introduced and through several rounds of screening molecules with higher affinity are selected. The *in vivo* tumor targeting was several times higher than the earlier affibody studied and clear visualization was obtained with γ -scintigraphy 1 h after injection (149). There has also been success at producing a completely synthetic affibody to which a chelating agent for complexing with radiometals was added (148). When this higher affinity affibody was radiolabeled with ^{111}In and administered to tumor bearing mice for evaluation, tumor targeting was comparable to that reported earlier. However, and not surprising, when a radiometal is used to label a molecule with $M_r < 60$ kDa, the radioactivity in the kidneys was appreciably higher (24, 150). However, this is not viewed as an insurmountable setback for affibodies in the arena of targeted radiation therapy. An affibody labeled with a radiometal would have potential in locoregional administration for the treatment of cancers confined to anatomical regions, for example, ovarian cancer, urinary bladder cancer, or primary brain tumors. Affibodies, with their very rapid pharmacokinetics and ability to penetrate tumors, may also have potential as delivery vehicles for short-lived radionuclides such as ^{212}Bi ($t_{1/2} = 60.6$ min), ^{213}Bi ($t_{1/2} = 45.6$ min), ^{211}At ($t_{1/2} = 7.2$ h), or even ^{212}Pb ($t_{1/2} = 10.6$ h). The ability to introduce residues for site-specific modifications, that is, conjugation with a bifunctional chelate, for

complexing radiometals provides a well-defined radiopharmaceutical that is homogeneous (151).

1.11 OTHER STRATEGIES

Rapid clearance from the blood along with tumor penetration has been achieved with molecules such as the scFvs, Fabs, diabodies, and other MAb-based forms. Those properties though, as indicated throughout this chapter, have required compromises and have come at a cost. As indicated when discussing each of these molecules, reducing the size of a protein to less than 60 kDa results in their elimination through renal filtration, and when conjugated with a radionuclide, there is a concomitant increase in the radiation doses to the kidneys. Aside from increasing the size/valency of the engineered antibody fragments by tethering fragments together, a number of strategies have been taken to increase the size and/or circulation time of smaller MAb variants. The approaches have been to modify fragments, either chemically or by genetic engineering with, for example, albumin, the Fc domain of antibodies, or polyethylene glycol.

1.11.1 Fc Domain and the Neonatal Fc Receptor

The Fc domain of an Ig is responsible for its retention in the blood and as such offers the chance to manipulate the pharmacokinetics of an antibody. Interactions of the Fc domain with the neonatal Fc receptor (FcRn) protect Igs (IgGs) from degradation by lysosomes, such that the FcRn is attributed with maintaining IgG levels in the blood (58). Igs are taken up by vascular endothelial cells by endocytosis and transported to early endosomes where the FcRn is also located. Under slightly acidic conditions ($\text{pH} < 6.5$), IgG will bind to the FcRn with high affinity; low-affinity binding occurs under neutral conditions (152). IgGs that are bound to FcRn will be transported back to the circulation or transported across the endothelial cell and released into the interstitial fluids. The neutral pH of the fluids in either location triggers the dissociation of the IgG from FcRn. Three amino acids that are conformationally in close proximity, an Ile and a His in the C_{H2} domain and a His in the C_{H3} domain, are required for IgG binding with the FcRn. Mutations of any of these three residues results in an abbreviated serum half-life of the IgG (153). Conversely, residue mutations near the FcRn binding site can increase the binding affinity for the receptor, resulting in an IgG with a longer retention time in the serum (154). These studies provided the basis for Kenanova et al. (155) to engineer a single-chain Fv-Fc fragment and five variants with the objective of modulating the serum half-life of an scFv and tailoring molecules for specific applications (Fig. 1.5). Biodistribution studies in mice proved that tumor targeting molecules could be produced that varied in serum half-lives ranging from 8 h to 12 days (155). Tumor targeting was visualized with the anti-CEA scFv-Fc variants using a microPET scanner. Images with high signal-to-noise background were obtained ~18 h post-injection of the ¹²⁴I-labeled scFv-Fc variants; the variant with the fastest serum pharmacokinetics produced the

earliest image. The pH sensitivity of the Fc–FcRn interaction provided the rationale for the mutations that were inserted into the Fc domain. For example, at an acidic pH, the His residue is positively charged; an Arg was substituted to maintain this positive charge. What was of further consideration was that Arg would also be positively charged in the more neutral milieu of the serum, interstitial fluids, or endosomes, thus discouraging dissociation of the scFv-Fc from the FcRn (155). A His substituted with a glutamine resulted in the variant having the shortest residence time in the serum; Gln remains uncharged in acidic or neutral backgrounds. When both histidines in the FcRn binding site of the Fc were modified, the resulting variant demonstrated the greatest reduction in serum retention of all of the variants.

Three of the anti-CEA scFv-Fc variants underwent further evaluation to assess their potential in radioimmunotherapy regimens (156). Not surprising, *in vivo* studies indicate that there is an inverse relationship between residence time in the blood and tumor uptake of the radiolabeled scFv-Fc. However, even the variant with the fastest clearance from the blood demonstrated good tumor targeting. Renal accretion of radioactivity is not an issue with these molecules since they were engineered to exceed the molecular weight threshold for clearance through the kidneys. Hepatic uptake was observed when the scFv-Fc variants were labeled with ^{111}In ; this was comparable with that observed for a minibody of the same MAb (T84.66) (117). Due to this hepatic uptake in three mouse models, the investigators argued that if the fastest clearing variant (both histidines substituted) were labeled with ^{90}Y , dosimetry estimates indicated that the liver would receive a similar radiation absorbed dose as the tumor (156). The scFv-Fc would be a more appropriate agent for targeted radiation therapy if radiolabeled with ^{131}I , due to the catabolism and elimination of radioiodine and the absence of its sequestration in the liver. It is also suggested that this particular molecule would have applications in multistep approaches that employ bispecific forms for pretargeting.

The data gathered from biodistribution studies in which mice were coinjected with anti-CEA scFv-Fc constructs labeled with ^{111}In and ^{125}I have allowed investigators to develop a physiologically based pharmacokinetic model that can simulate the *in vivo* behavior of an scFv-Fc labeled with either ^{111}In or radioiodine. This model will prove quite useful in designing antibody-based therapeutics as well as assist in establishing dosing schedules for patients in the clinic by translating preclinical animal data to humans (157).

Production of recombinant MAb forms does not always go smoothly or as planned. The scFv-Fc molecules can self-assemble into multimeric forms. An anti-CD20 scFv-Fc was generated for evaluation as an immunotherapeutic and/or radioimmunotherapeutic agent. The purified product contained not only the expected monomeric form of 104 kDa but also discrete multiple species of incrementally higher molecular weights based on the size of the single unit (158). This particular scFv-Fc demonstrated a propensity for multimerization that appeared to be driven by intermolecular pairing of variable regions of an scFv-Fc. Systematically, this group demonstrated that in this particular case, it was not the linker they had chosen nor was it interactions due to the hinge region of the molecule. The investigators postulated that during production of an anti-CD20 scFv-Fc, the variable domains of the nascent polypeptides are

juxtaposed as they are synthesized with the domains of another strand. Further investigation of suspect residues that interact at the V_L - V_H interface or in the framework that affect folding or to identify residues that become available for chain-chain interactions is warranted. Elucidation of such factors would provide critical information for the design and production of future scFv-Fc molecules as well as other recombinant MAb base molecules.

1.11.2 PEGylation

Conjugation of proteins with polyethylene glycol has been shown to minimize or abrogate the immunogenicity of a protein and to increase its residence time in the circulation (159–162). In addition, PEGylation of the smaller scFv provides yet another method of increasing their size to avoid renal accumulation of radioactivity when conjugated with radiometals.

Random conjugation of scFvs with PEG has been demonstrated to be effective. PEGylation of CC49 scFv with increasing sizes of PEG (molecular masses ranging from 2000 to 20,000 Da) yielded conjugates with corresponding increasing half-lives in the serum (163). The caveat to this PEGylation was that careful adjustments to the reaction were required to ensure that the final product had a PEG:scFv ratio no greater than 2; loss of immunoreactivity was noted at higher ratios. These studies also illustrated the requirement for careful consideration of the chemistry employed for the PEGylation, that is, employing carboxylic or amine moieties. Immunoreactivity of the scFv was influenced by the chemical route chosen. Interestingly, it was determined that the length of the PEG polymer was more effective in prolonging the serum half-life of the conjugate than did an increase in the total mass of PEG.

In another study, an anti-CEA diabody was coupled with PEG, conjugated with cysteinyl-DOTA and labeled with ^{111}In (164). With an apparent molecular weight of 75,000 Da, the radiolabeled PEG-diabody retained immunoreactivity. Compared to the unmodified diabody, tumor uptake was greatly improved at early time points and was retained at higher levels for a longer period. Renal uptake was reduced by ~ 2.5 -fold but was still high with $\sim 50\%$ ID/g at 24 h. An increase in hepatic uptake was also observed. The PEG was effective in improving the tumor uptake, a function of the longer circulation time; however, the renal uptake still remained an obstacle to using this MAb form for RIT, restricting its use as a delivery vehicle for the radioiodines or α -particle emitters.

As discussed, the random conjugation of a molecule with PEG can affect its bioactivity, which therefore requires testing. Efficiency of these reactions will vary from batch-to-batch as will the number of PEG molecules that will be attached per protein molecule. The conjugation invariably results in a heterogeneous product that is difficult to characterize and therefore problematic to standardize for a potential pharmaceutical product (165–167). A solution to these obstacles is the insertion of amino acids for the purpose of performing site-specific conjugations. Recent work has taken the approach of introducing unpaired cysteine residues in the scFv construct to provide a specific site for PEGylation with the goal of preserving the immunoreactivity of the di-scFv (168). First, a systematic investigation of the appropriate length of the

peptide linker determined that a 20-amino acid linker resulted in the best production yield of an anti-MUC-1 di-scFv. Again, the G₄S repeat was chosen based on the flexibility and hydrophilicity it provides to the molecule along with its low immunogenicity (169). A comparison of an anti-MUC-1 di-scFv with a cysteine introduced at five locations within the molecule led to the identification of a form that retained immunoreactivity. Although all five versions were reactive with the cognate antigen, some differences were discernible. However, the cysteine location seemed to have a greater effect on the efficiency of the PEGylation. The highest PEGylation efficiency occurred when the available cysteine was located in the inter-scFv linker. It was also reported that PEG of various sizes (up to 40 kDa) could be conjugated to the di-scFv without loss of immunoreactivity.

1.11.3 Albumin Binding

Human serum albumin (HSA), the most abundant protein in the blood plasma, serves as a transporter and scavenger (i.e., fatty acids, bilirubin, anions) for an assortment of molecules. Binding with albumin (i) increases the solubility of a molecule in the plasma, (ii) provides protection from oxidation/degradation, and (iii) lowers the toxicity of a molecule (170). HSA interacts reversibly with a wide spectrum of drugs with varying affinity; valproate, warfarin, ibuprofen, and indomethacin are some examples. More importantly, with a 19-day half-life, albumin can significantly prolong the circulating time of a drug. In fact, binding with albumin has become a common strategy for altering the pharmacokinetics of small molecular weight drugs such as analogues of insulin (171). Associating albumin with immunoglobulin has been evaluated using three tactics: chemical conjugation, genetic fusion, and creation of a bifunctional molecule with albumin and antigen binding capabilities (Fig. 1.5) (172). All three methods are successful in generating molecules that retain reactivity with antigen and also have an extended residence time in the plasma. A chemical conjugation of a Fab' with HSA exploits the exposed cysteine in the former with the free cysteine of the latter. The proteins are subjected to reduction with reagents, combined, and then the reducing agents removed to allow disulfide bond formation to occur between the two proteins. Such a conjugate was created with an anti-TNF Fab fragment and HSA. Compared to the Fab' alone, the addition of the HSA increased the $t_{1/2\alpha}$ plasma pharmacokinetics from 1 to 4.6 h while the $t_{1/2\beta}$ increased from 31.4 to 39.6 h. The conjugation, however, is not very efficient (a 5% yield was reported) and even when optimized resulted in a heterogeneous mixture requiring several purification steps and a product that would not contain a uniform ratio of Fab to HSA (172). Fusion proteins consisting of an antibody fragment and HSA eliminate the difficulties just mentioned and provide a uniform product that can be well characterized. The scFv of an antibody is either fused directly to the N-terminus of HSA, or linkers such as (Gly)₄-Ser repeats are inserted between the two as spacers, providing some flexibility to the fusion protein and avoiding steric hindrance. The *in vivo* evaluation of these fusion proteins has indicated that in a biphasic analysis, their plasma clearance is similar to that of HSA and was found to have a considerably longer retention time in the plasma than that reported for an

scFv (22, 172, 173). As mentioned previously, unacceptably high accretion in the kidneys and liver is observed when sFv fragments, diabodies, and minibodies are labeled with radiometals (24, 117). High renal and hepatic accumulation of radioactivity has not been evident with an ^{111}In -labeled fusion protein consisting of an scFv and HSA (173).

A bifunctional molecule, produced either by chemical methods or through genetic engineering, that would bind a target antigen and albumin represents another means of recruiting albumin. In one instance, the Fab' of an anti-rat serum albumin (RSA) antibody was cross-linked with the Fab' of an anti-TNF antibody (172). The resulting F(ab')₂ demonstrated reactivity with both TNF and RSA. More importantly, the bispecific F(ab')₂ had a 6.6- and 2.2-fold increase in the $t_{1/2\beta}$ plasma clearance phase compared to a control F(ab')₂ and RSA, respectively. This approach has been taken one step further with the creation of multivalent fusion proteins constructed from nanobodies. One such fusion protein contained two nanobodies with specificity for EGFR and a third was reactive with albumin (174). The bispecific nanobody was radiolabeled with ^{177}Lu and evaluated in a tumor bearing mouse model. Excellent tumor targeting, comparable to cetuximab, was achieved while modest uptake of radioactivity was observed in the kidneys. The fusion protein was also shown by immunohistochemical analysis to penetrate tumor tissue.

Another interesting approach borrows from the fact that albumin contains several domains that bind to small molecules and metal ions (171). Using phage display techniques, a library of high-affinity albumin binding peptides was developed (175). Peptides that bound rat, human, and rabbit albumin were synthesized and characterized. Based on favorable pharmacokinetics and stability, two peptides were chosen and recombinantly fused with a Fab fragment. In an elegant set of studies, these investigators demonstrated high-affinity binding of the Fab fusion protein with albumin as well as binding with the cognate antigen. The half-life of the molecule was increased ~40-fold. Having demonstrated proof of concept, this tactic was then translated to trastuzumab (Herceptin), the anti-HER2 MAb currently used for treatment of metastatic breast cancer patients (176, 177).

Several variants of a trastuzumab Fab with the albumin binding peptide (AB.Fab) were generated and evaluated for albumin and HER2 binding. Variations consisted of introducing a peptide linker (Gly₃Ser) or altering the length of the albumin binding peptide (177). The variant with the linker sequence exhibited a higher affinity for albumin, maintained its reactivity with HER2, and had a prolonged retention in the plasma. Compared to the Herceptin Fab, the $t_{1/2\beta}$ in mice, rats, and rabbits was extended by 15.4-, 21.0-, and 11.5-fold, respectively (176, 177). Tumor targeting was visualized and quantitated by SPECT and CT (176). The AB.Fab resulted in a more rapid uptake in the tumor, which at 48 h was comparable to intact trastuzumab IgG and ~4-fold greater than the Fab fragment. The AB.Fab cleared from the blood rapidly and did not appear to accumulate in the kidneys. Greater uniformity of distribution through tumor tissue was evident by histological analysis of HER2-positive tumor xenografts. These properties of the AB.Fab indicate that these fusion proteins may be effective vehicles for the delivery of therapeutic doses of radiation in RIT applications. The ability to select a peptide that has relevance for humans and yet be characterized in

another species can facilitate its translation to clinical trials with cancer patients. These studies illustrate the exquisite fine-tuning that can be performed to obtain a targeting molecule of the desired properties.

1.12 CONCLUDING REMARKS

This chapter has presented an overview of various forms of MAb and their application in targeted radiotherapy of cancer. RIT still offers the potential of delivering a high radiation absorbed dose that is tumor selective with modest to tolerable, and in some cases minimal, damage to normal tissues. The clinical RIT trials with murine monoclonal antibodies identified a number of obstacles to effective treatment, which included inadequate delivery of a therapeutic dose to and throughout the tumor, bone marrow toxicity, and the development of human anti-mouse antibodies. Genetic engineering has greatly facilitated our ability to address these challenges. The antigen binding, specificity, affinity, and *in vivo* characteristics of a MAb can be optimized. Recombinant technology has also shown us the compromises of antibody-based therapy of cancer. There are a myriad of MAb forms and treatment strategies to evaluate. The availability of targeted radiation therapy provides a viable alternative for the treatment of cancer patients.

REFERENCES

1. Bale WF, Spar IL, Goodland RL. Experimental radiation therapy of tumors with I^{131} -carrying antibodies to fibrin. *Cancer Res* 1960;20:1488–1494.
2. Pressman D. The development and use of radiolabeled antitumor antibodies. *Cancer Res* 1980;40:2960–2964.
3. Hiramoto R, Yagi Y, Pressman D. *In vivo* fixation of antibodies in the adrenal. *Proc Soc Exp Biol Med* 1958;98:870–874.
4. McCardle RJ, Harper PV, Spar IL, Bale WF, Andros G, Jiminez F. Studies with iodine-131-labeled antibody to human fibrinogen for diagnosis and therapy of tumors. *J Nucl Med* 1966;7:837–847.
5. Ehrlich P, Herta C, Shigas K. Ueber einige verwendungen der naphthochinosulfsaure. *Ztschr f Physiol Chem* 1904;61:379–392.
6. Kohler G, Milstein C. Continuous cultures of fused cells secreting antibody of predefined specificity. *Nature* 1975;256:495–497.
7. Knox SJ, Meredith RF. Clinical radioimmunotherapy. *Semin Radiat Oncol* 2000;10:73–93.
8. Jurcic JG, Scheinberg DA. Radioimmunotherapy of hematological cancer: problems and progress. *Clin Cancer Res* 1995;1:1439–1446.
9. Schlom J. Monoclonal antibodies: they're more and less than you think. In: Broder S, editor. *Molecular Foundations of Oncology*. Williams and Wilkins, Baltimore, MD, 1990.
10. Reichert JM, Wenger JB. Development trends for new cancer therapeutics and vaccines. *Drug Discov Today* 2008;13:30–37.

11. Witzig TE. The use of ibritumomab tiuxetan radioimmunotherapy for patients with relapsed B-cell non-Hodgkin's lymphoma. *Semin Oncol* 2000;27:74–78.
12. Vose JM. Bexxar: novel radioimmunotherapy for the treatment of low-grade and transformed low-grade non-Hodgkin's lymphoma. *Oncologist* 2004;9:160–172.
13. Khazaeli MB, Conry RM, LoBuglio AF. Human immune response to monoclonal antibodies. *J Immunother* 1994;15:42–52.
14. Tamura M, Milenic DE, Iwahashi M, Padlan E, Schlom J, Kashmiri SV. Structural correlates of an anticarcinoma antibody: identification of specificity-determining residues (SDRs) and development of a minimally immunogenic antibody variant by retention of SDRs only. *J Immunol* 2000;164:1432–1441.
15. Blanco I, Kawatsu R, Harrison K, et al. Antiidiotypic response against murine monoclonal antibodies reactive with tumor-associated antigen TAG-72. *J Clin Immunol* 1997;17:96–106.
16. Milenic DE, Esteban JM, Colcher D. Comparison of methods for the generation of immunoreactive fragments of a monoclonal antibody (B72.3) reactive with human carcinomas. *J Immunol Methods* 1989;120:71–83.
17. Parham P, Androlewicz MJ, Brodsky FM, Holmes NJ, Ways JP. Monoclonal antibodies: purification, fragmentation and application to structural and functional studies of class I MHC antigens. *J Immunol Methods* 1982;53:133–173.
18. Waller M, Curry N, Mallory J. Immunochemical and serological studies of enzymatically fractionated human IgG globulins. I. Hydrolysis with pepsin, papain, ficin and bromelin. *Immunochemistry* 1968;5:577–583.
19. Juweid ME, Hajjar G, Swayne LC, et al. Phase I/II trial of ¹³¹I-MN-14F(ab)₂ anti-carcinoembryonic antigen monoclonal antibody in the treatment of patients with metastatic medullary thyroid carcinoma. *Cancer* 1999;85:1828–1842.
20. Lane DM, Eagle KF, Begent RH, et al. Radioimmunotherapy of metastatic colorectal tumours with iodine-131-labelled antibody to carcinoembryonic antigen: phase I/II study with comparative biodistribution of intact and F(ab')₂ antibodies. *Br J Cancer* 1994;70:521–525.
21. Yokota T, Milenic DE, Whitlow M, Schlom J. Rapid tumor penetration of a single-chain Fv and comparison with other immunoglobulin forms. *Cancer Res* 1992;52:3402–3408.
22. Milenic DE, Yokota T, Filpula DR, et al. Construction, binding properties, metabolism, and tumor targeting of a single-chain Fv derived from the pancarcinoma monoclonal antibody CC49. *Cancer Res* 1991;51:6363–6371.
23. Carrasquillo JA, Krohn KA, Beaumier P, et al. Diagnosis of and therapy for solid tumors with radiolabeled antibodies and immune fragments. *Cancer Treat Rep* 1984;68:317–328.
24. Schott ME, Milenic DE, Yokota T, et al. Differential metabolic patterns of iodinated versus radiometal chelated anticarcinoma single-chain Fv molecules. *Cancer Res* 1992;52:6413–6417.
25. Yokota T, Milenic DE, Whitlow M, Wood JF, Hubert SL, Schlom J. Microautoradiographic analysis of the normal organ distribution of radioiodinated single-chain Fv and other immunoglobulin forms. *Cancer Res* 1993;53:3776–3783.
26. Behr TM, Sharkey RM, Juweid ME, et al. Reduction of the renal uptake of radiolabeled monoclonal antibody fragments by cationic amino acids and their derivatives. *Cancer Res* 1995;55:3825–3834.

27. DePalatis LR, Frazier KA, Cheng RC, Kotite NJ. Lysine reduces renal accumulation of radioactivity associated with injection of the [¹⁷⁷Lu]alpha-[2-(4-aminophenyl) ethyl]-1,4,7,10-tetraaza-cyclodecane-1,4,7,10-tetraacetic acid-CC49 Fab radioimmunoconjugate. *Cancer Res* 1995;55:5288–5295.
28. Morrison S, Schlom J. Recombinant chimeric monoclonal antibodies. In: DeVita V, Rosenberg S, editors. *Important Advances in Oncology*. JB Lippincott, Philadelphia, PA, 1990, pp. 3–18.
29. Hiatt A, Cafferkey R, Bowdish K. Production of antibodies in transgenic plants. *Nature* 1989;342:76–78.
30. LoBuglio AF, Wheeler RH, Trang J, et al. Mouse/human chimeric monoclonal antibody in man: kinetics and immune response. *Proc Natl Acad Sci USA* 1989;86:4220–4224.
31. Baeuerle PA, Gires O. EpCAM (CD326) finding its role in cancer. *Br J Cancer* 2007;96:417–423.
32. Litvinov SV, Bakker HA, Gourevitch MM, Velders MP, Warnaar SO. Evidence for a role of the epithelial glycoprotein 40 (Ep-CAM) in epithelial cell–cell adhesion. *Cell Adhes Commun* 1994;2:417–428.
33. Meredith RF, Khazaeli MB, Grizzle WE, et al. Direct localization comparison of murine and chimeric B72.3 antibodies in patients with colon cancer. *Hum Antibodies Hybridomas* 1993;4:190–197.
34. Maloney DG, Grillo-Lopez AJ, White CA, et al. IDEC-C2B8 (Rituximab) anti-CD20 monoclonal antibody therapy in patients with relapsed low-grade non-Hodgkin's lymphoma. *Blood* 1997;90:2188–2195.
35. Jones PT, Dear PH, Foote J, Neuberger MS, Winter G. Replacing the complementarity-determining regions in a human antibody with those from a mouse. *Nature* 1986;321:522–525.
36. Padlan EA. Anatomy of the antibody molecule. *Mol Immunol* 1994;31:169–217.
37. Amit AG, Mariuzza RA, Phillips SE, Poljak RJ. Three-dimensional structure of an antigen–antibody complex at 2.8 Å resolution. *Science* 1986;233:747–753.
38. Kashmiri SV, De Pascalis R, Gonzales NR. Developing a minimally immunogenic humanized antibody by SDR grafting. *Methods Mol Biol* 2004;248:361–376.
39. Kashmiri SV, Shu L, Padlan EA, Milenic DE, Schlom J, Hand PH. Generation, characterization, and *in vivo* studies of humanized anticarcinoma antibody CC49. *Hybridoma* 1995;14:461–473.
40. Winter G, Harris WJ. Humanized antibodies. *Immunol Today* 1993;14:243–246.
41. Riechmann L, Clark M, Waldmann H, Winter G. Reshaping human antibodies for therapy. *Nature* 1988;332:323–327.
42. Caron PC, Schwartz MA, Co MS, et al. Murine and humanized constructs of monoclonal antibody M195 (anti-CD33) for the therapy of acute myelogenous leukemia. *Cancer* 1994;73:1049–1056.
43. Sharkey RM, Juweid M, Shevitz J, et al. Evaluation of a complementarity-determining region-grafted (humanized) anti-carcinoembryonic antigen monoclonal antibody in preclinical and clinical studies. *Cancer Res* 1995;55:5935s–5945s.
44. Kramer EL, Liebes L, Wasserheit C, et al. Initial clinical evaluation of radiolabeled MX-DTPA humanized BrE-3 antibody in patients with advanced breast cancer. *Clin Cancer Res* 1998;4:1679–1688.

45. Caron PC, Jurcic JG, Scott AM, et al. A phase 1B trial of humanized monoclonal antibody M195 (anti-CD33) in myeloid leukemia: specific targeting without immunogenicity. *Blood* 1994;83:1760–1768.
46. Schneider WP, Glaser SM, Kondas JA, Hakimi J. The anti-idiotypic response by cynomolgus monkeys to humanized anti-Tac is primarily directed to complementarity-determining regions H1, H2, and L3. *J Immunol* 1993;150:3086–3090.
47. Singer II, Kawka DW, DeMartino JA, et al. Optimal humanization of 1B4, an anti-CD18 murine monoclonal antibody, is achieved by correct choice of human V-region framework sequences. *J Immunol* 1993;150:2844–2857.
48. Stephens S, Emtage S, Vetterlein O, et al. Comprehensive pharmacokinetics of a humanized antibody and analysis of residual anti-idiotypic responses. *Immunology* 1995;85:668–674.
49. Pendley C, Schantz A, Wagner C. Immunogenicity of therapeutic monoclonal antibodies. *Curr Opin Mol Ther* 2003;5:172–179.
50. Nanus DM, Milowsky MI, Kostakoglu L, et al. Clinical use of monoclonal antibody HuJ591 therapy: targeting prostate specific membrane antigen. *J Urol* 2003;170: S84–S88; discussion S88–S89.
51. Smith-Jones PM. Radioimmunotherapy of prostate cancer. *Q J Nucl Med Mol Imaging* 2004;48:297–304.
52. Mulligan T, Carrasquillo JA, Chung Y, et al. Phase I study of intravenous Lu-labeled CC49 murine monoclonal antibody in patients with advanced adenocarcinoma. *Clin Cancer Res* 1995;1:1447–1454.
53. Iwahashi M, Milenic DE, Padlan EA, Bei R, Schlom J, Kashmiri SV. CDR substitutions of a humanized monoclonal antibody (CC49): contributions of individual CDRs to antigen binding and immunogenicity. *Mol Immunol* 1999;36:1079–1091.
54. Padlan EA, Abergel C, Tipper JP. Identification of specificity-determining residues in antibodies. *FASEB J* 1995;9:133–139.
55. Kashmiri SV, Iwahashi M, Tamura M, Padlan EA, Milenic DE, Schlom J. Development of a minimally immunogenic variant of humanized anti-carcinoma monoclonal antibody CC49. *Crit Rev Oncol Hematol* 2001;38:3–16.
56. De Pascalis R, Gonzales NR, Padlan EA, et al. *In vitro* affinity maturation of a specificity-determining region-grafted humanized anticarcinoma antibody: isolation and characterization of minimally immunogenic high-affinity variants. *Clin Cancer Res* 2003;9:5521–5531.
57. De Pascalis R, Iwahashi M, Tamura M, et al. Grafting of “abbreviated” complementarity-determining regions containing specificity-determining residues essential for ligand contact to engineer a less immunogenic humanized monoclonal antibody. *J Immunol* 2002;169:3076–3084.
58. Waldmann TA, Strober W. Metabolism of immunoglobulins. *Prog Allergy* 1969;13:1–110.
59. Shuke N, Steis R, McCabe R. Pharmacokinetics of two human IgM monoclonal antibodies (16.88 and 28A32). *J Nucl Med* 1989;30:909.
60. Cole SP, Vreeken EH, Roder JC. Antibody production by human X human hybridomas in serum-free medium. *J Immunol Methods* 1985;78:271–278.
61. Green LL, Hardy MC, Maynard-Currie CE, et al. Antigen-specific human monoclonal antibodies from mice engineered with human Ig heavy and light chain YACs. *Nat Genet* 1994;7:13–21.

62. Lonberg N, Taylor LD, Harding FA, et al. Antigen-specific human antibodies from mice comprising four distinct genetic modifications. *Nature* 1994;368:856–859.
63. Lonberg N. Human antibodies from transgenic animals. *Nat Biotechnol* 2005; 23:1117–1125.
64. Tomizuka K, Shinohara T, Yoshida H, et al. Double trans-chromosomal mice: maintenance of two individual human chromosome fragments containing Ig heavy and kappa loci and expression of fully human antibodies. *Proc Natl Acad Sci USA* 2000;97:722–727.
65. McCafferty J, Griffiths AD, Winter G, Chiswell DJ. Phage antibodies: filamentous phage displaying antibody variable domains. *Nature* 1990;348:552–554.
66. Rajpal A, Beyaz N, Haber L, et al. A general method for greatly improving the affinity of antibodies by using combinatorial libraries. *Proc Natl Acad Sci USA* 2005; 102:8466–8471.
67. Lonberg N. Fully human antibodies from transgenic mouse and phage display platforms. *Curr Opin Immunol* 2008.
68. Foon KA, Yang XD, Weiner LM, et al. Preclinical and clinical evaluations of ABX-EGF, a fully human anti-epidermal growth factor receptor antibody. *Int J Radiat Oncol Biol Phys* 2004;58:984–990.
69. Rowinsky EK, Schwartz GH, Gollob JA, et al. Safety, pharmacokinetics, and activity of ABX-EGF, a fully human anti-epidermal growth factor receptor monoclonal antibody in patients with metastatic renal cell cancer. *J Clin Oncol* 2004;22:3003–3015.
70. Hamers-Casterman C, Atarhouch T, Muyldermans S, et al. Naturally occurring antibodies devoid of light chains. *Nature* 1993;363:446–448.
71. Dumoulin M, Conrath K, Van Meirhaeghe A, et al. Single-domain antibody fragments with high conformational stability. *Protein Sci* 2002;11:500–515.
72. Revets H, De Baetselier P, Muyldermans S. Nanobodies as novel agents for cancer therapy. *Expert Opin Biol Ther* 2005;5:111–124.
73. Joosten V, Lokman C, Van Den Hondel CA, Punt PJ. The production of antibody fragments and antibody fusion proteins by yeasts and filamentous fungi. *Microb Cell Fact* 2003;2:1.
74. Gaikam LO, Huang L, Caveliers V, et al. Comparison of the biodistribution and tumor targeting of two ^{99m}Tc-labeled anti-EGFR nanobodies in mice, using pinhole SPECT/micro-CT. *J Nucl Med* 2008;49:788–795.
75. Cortez-Retamozo V, Lauwereys M, Hassanzadeh GhG, et al. Efficient tumor targeting by single-domain antibody fragments of camels. *Int J Cancer* 2002;98:456–462.
76. Gillies SD, Wesolowski JS. Antigen binding and biological activities of engineered mutant chimeric antibodies with human tumor specificities. *Hum Antibodies Hybridomas* 1990;1:47–54.
77. Dorai H, Mueller BM, Reisfeld RA, Gillies SD. Aglycosylated chimeric mouse/human IgG1 antibody retains some effector function. *Hybridoma* 1991;10:211–217.
78. Mueller BM, Romerdahl CA, Gillies SD, Reisfeld RA. Enhancement of antibody-dependent cytotoxicity with a chimeric anti-GD2 antibody. *J Immunol* 1990; 144:1382–1386.
79. Slavin-Chiorini DC, Horan Hand PH, Kashmiri SV, Calvo B, Zaremba S, Schlom J. Biologic properties of a C_H2 domain-deleted recombinant immunoglobulin. *Int J Cancer* 1993;53:97–103.

80. Slavin-Chiorini DC, Kashmiri SV, Lee HS, et al. A CDR-grafted (humanized) domain-deleted antitumor antibody. *Cancer Biother Radiopharm* 1997;12:305–316.
81. Slavin-Chiorini DC, Kashmiri SV, Schlom J, et al. Biological properties of chimeric domain-deleted anticarcinoma immunoglobulins. *Cancer Res* 1995;55:5957s–5967s.
82. Milenic D, Garmestani K, Dadachova E, et al. Radioimmunotherapy of human colon carcinoma xenografts using a ^{213}Bi -labeled domain-deleted humanized monoclonal antibody. *Cancer Biother Radiopharm* 2004;19:135–147.
83. Rogers BE, Roberson PL, Shen S, et al. Intraperitoneal radioimmunotherapy with a humanized anti-TAG-72 (CC49) antibody with a deleted $\text{C}_{\text{H}2}$ region. *Cancer Biother Radiopharm* 2005;20:502–513.
84. Forero A, Meredith RF, Khazaeli MB, et al. A novel monoclonal antibody design for radioimmunotherapy. *Cancer Biother Radiopharm* 2003;18:751–759.
85. Xiao J, Horst S, Hinkle G, et al. Pharmacokinetics and clinical evaluation of ^{125}I -radiolabeled humanized CC49 monoclonal antibody (HuCC49 $\Delta\text{C}_{\text{H}2}$) in recurrent and metastatic colorectal cancer patients. *Cancer Biother Radiopharm* 2005;20:16–26.
86. Glaser SM, Hughes IE, Hopp JR, Hathaway K, Perret D, Reff ME. Novel antibody hinge regions for efficient production of $\text{C}_{\text{H}2}$ domain-deleted antibodies. *J Biol Chem* 2005;280:41494–41503.
87. Sivolapenko GB, Douli V, Pectasides D, et al. Breast cancer imaging with radiolabelled peptide from complementarity-determining region of antitumour antibody. *Lancet* 1995;346:1662–1666.
88. Williams WV, Kieber-Emmons T, VonFeldt J, Greene MI, Weiner DB. Design of bioactive peptides based on antibody hypervariable region structures. Development of conformationally constrained and dimeric peptides with enhanced affinity. *J Biol Chem* 1991;266:5182–5190.
89. Bird RE, Hardman KD, Jacobson JW, et al. Single-chain antigen-binding proteins. *Science* 1988;242:423–426.
90. Skerra A, Pluckthun A. Assembly of a functional immunoglobulin Fv fragment in *Escherichia coli*. *Science* 1988;240:1038–1041.
91. Azuma T, Hamaguchi K, Migita S. Interactions between immunoglobulin polypeptide chains. *J Biochem* 1974;76:685–693.
92. Glockshuber R, Malia M, Pfitzinger I, Pluckthun A. A comparison of strategies to stabilize immunoglobulin Fv-fragments. *Biochemistry* 1990;29:1362–1367.
93. Horne C, Klein M, Polidoulis I, Dorrington KJ. Noncovalent association of heavy and light chains of human immunoglobulins. III. Specific interactions between V_{H} and V_{L} . *J Immunol* 1982;129:660–664.
94. Ward ES, Gussow D, Griffiths AD, Jones PT, Winter G. Binding activities of a repertoire of single immunoglobulin variable domains secreted from *Escherichia coli*. *Nature* 1989;341:544–546.
95. Huston JS, Levinson D, Mudgett-Hunter M, et al. Protein engineering of antibody binding sites: recovery of specific activity in an anti-digoxin single-chain Fv analogue produced in *Escherichia coli*. *Proc Natl Acad Sci USA* 1988;85:5879–5883.
96. Desplancq D, King DJ, Lawson AD, Mountain A. Multimerization behaviour of single chain Fv variants for the tumour-binding antibody B72.3. *Protein Eng* 1994; 7:1027–1033.

97. Power BE, Doughty L, Shapira DR, et al. Noncovalent scFv multimers of tumor-targeting anti-Lewis(y) hu3S193 humanized antibody. *Protein Sci* 2003;12:734–747.
98. Wu AM. Engineering multivalent antibody fragments for *in vivo* targeting. *Methods Mol Biol* 2004;248:209–225.
99. Colcher D, Bird R, Roselli M, et al. *In vivo* tumor targeting of a recombinant single-chain antigen-binding protein. *J Natl Cancer Inst* 1990;82:1191–1197.
100. McDevitt MR, Sgouros G, Finn RD, et al. Radioimmunotherapy with alpha-emitting nuclides. *Eur J Nucl Med* 1998;25:1341–1351.
101. Milenic DE, Brechbiel MW. Targeting of radio-isotopes for cancer therapy. *Cancer Biol Ther* 2004;3:361–370.
102. Wu AM, Chen W, Raubitschek A, et al. Tumor localization of anti-CEA single-chain Fvs: improved targeting by non-covalent dimers. *Immunotechnology* 1996;2:21–36.
103. Adams GP, Schier R, Marshall K, et al. Increased affinity leads to improved selective tumor delivery of single-chain Fv antibodies. *Cancer Res* 1998;58:485–490.
104. Adams GP, Schier R, McCall AM, et al. High affinity restricts the localization and tumor penetration of single-chain fv antibody molecules. *Cancer Res* 2001;61:4750–4755.
105. Larson SM, El-Shirbiny AM, Divgi CR, et al. Single chain antigen binding protein (sFv CC49): first human studies in colorectal carcinoma metastatic to liver. *Cancer* 1997;80:2458–2468.
106. Begent RH, Verhaar MJ, Chester KA, et al. Clinical evidence of efficient tumor targeting based on single-chain Fv antibody selected from a combinatorial library. *Nat Med* 1996;2:979–984.
107. Mayer A, Tsiompanou E, O'Malley D, et al. Radioimmunoguided surgery in colorectal cancer using a genetically engineered anti-CEA single-chain Fv antibody. *Clin Cancer Res* 2000;6:1711–1719.
108. Almog O, Benhar I, Vasmatis G, et al. Crystal structure of the disulfide-stabilized Fv fragment of anticancer antibody B1: conformational influence of an engineered disulfide bond. *Proteins* 1998;31:128–138.
109. Bin Song K, Won M, Meares CF. Expression of recombinant Lym-1 single-chain Fv in *Escherichia coli*. *Biotechnol Appl Biochem* 1998;28 (Pt 2): 163–167.
110. Li Q, Hudson W, Wang D, Berven E, Uckun FM, Kersey JH. Pharmacokinetics and biodistribution of radioimmunoconjugates of anti-CD19 antibody and single-chain Fv for treatment of human B-cell malignancy. *Cancer Immunol Immunother* 1998;47:121–130.
111. Rodrigues ML, Presta LG, Kotts CE, et al. Development of a humanized disulfide-stabilized anti-p185HER2 Fv-beta-lactamase fusion protein for activation of a cephalosporin doxorubicin prodrug. *Cancer Res* 1995;55:63–70.
112. Webber KO, Kreitman RJ, Pastan I. Rapid and specific uptake of anti-Tac disulfide-stabilized Fv by interleukin-2 receptor-bearing tumors. *Cancer Res* 1995;55:318–323.
113. Rajagopal V, Pastan I, Kreitman RJ. A form of anti-Tac(Fv) which is both single-chain and disulfide stabilized: comparison with its single-chain and disulfide-stabilized homologs. *Protein Eng* 1997;10:1453–1459.
114. Kobayashi H, Han ES, Kim IS, et al. Similarities in the biodistribution of iodine-labeled anti-Tac single-chain disulfide-stabilized Fv fragment and anti-Tac disulfide-stabilized Fv fragment. *Nucl Med Biol* 1998;25:387–393.

115. Holliger P, Prospero T, Winter G. "Diabodies": small bivalent and bispecific antibody fragments. *Proc Natl Acad Sci USA* 1993;90:6444–6448.
116. Whitlow M, Filpula D, Rollence ML, Feng SL, Wood JF. Multivalent Fvs: characterization of single-chain Fv oligomers and preparation of a bispecific Fv. *Protein Eng* 1994;7:1017–1026.
117. Yazaki PJ, Wu AM, Tsai SW, et al. Tumor targeting of radiometal labeled anti-CEA recombinant T84.66 diabody and t84.66 minibody: comparison to radioiodinated fragments. *Bioconjug Chem* 2001;12:220–228.
118. Adams GP, Schier R, McCall AM, et al. Prolonged *in vivo* tumour retention of a human diabody targeting the extracellular domain of human HER2/neu. *Br J Cancer* 1998;77:1405–1412.
119. Beresford GW, Pavlinkova G, Booth BJ, Batra SK, Colcher D. Binding characteristics and tumor targeting of a covalently linked divalent CC49 single-chain antibody. *Int J Cancer* 1999;81:911–917.
120. Denton G, Brady K, Lo BK, et al. Production and characterization of an anti-(MUC1 mucin) recombinant diabody. *Cancer Immunol Immunother* 1999;48:29–38.
121. Adams GP, Shaller CC, Chappell LL, et al. Delivery of the alpha-emitting radioisotope bismuth-213 to solid tumors via single-chain Fv and diabody molecules. *Nucl Med Biol* 2000;27:339–346.
122. Robinson MK, Shaller C, Garmestani K, et al. Effective treatment of established human breast tumor xenografts in immunodeficient mice with a single dose of the alpha-emitting radioisotope astatine-211 conjugated to anti-HER2/neu diabodies. *Clin Cancer Res* 2008;14:875–882.
123. Adams GP, Shaller CC, Dadachova E, et al. A single treatment of yttrium-90-labeled CHX-A"-C6.5 diabody inhibits the growth of established human tumor xenografts in immunodeficient mice. *Cancer Res* 2004;64:6200–6206.
124. Whitlow M, Bell BA, Feng SL, et al. An improved linker for single-chain Fv with reduced aggregation and enhanced proteolytic stability. *Protein Eng* 1993;6:989–995.
125. Kostelny SA, Cole MS, Tso JY. Formation of a bispecific antibody by the use of leucine zippers. *J Immunol* 1992;148:1547–1553.
126. Pack P, Pluckthun A. Miniantibodies: use of amphipathic helices to produce functional, flexibly linked dimeric FV fragments with high avidity in *Escherichia coli*. *Biochemistry* 1992;31:1579–1584.
127. Ridgway JB, Presta LG, Carter P. 'Knobs-into-holes' engineering of antibody CH3 domains for heavy chain heterodimerization. *Protein Eng* 1996;9:617–621.
128. Pavlinkova G, Beresford G, Booth BJ, Batra SK, Colcher D. Charge-modified single chain antibody constructs of monoclonal antibody CC49: generation, characterization, pharmacokinetics, and biodistribution analysis. *Nucl Med Biol* 1999;26:27–34.
129. Goel A, Colcher D, Baranowska-Kortylewicz J, et al. Genetically engineered tetravalent single-chain Fv of the pancreatic carcinoma monoclonal antibody CC49: improved biodistribution and potential for therapeutic application. *Cancer Res* 2000;60:6964–6971.
130. Wittel UA, Jain M, Goel A, Chauhan SC, Colcher D, Batra SK. The *in vivo* characteristics of genetically engineered divalent and tetravalent single-chain antibody constructs. *Nucl Med Biol* 2005;32:157–164.

131. Chauhan SC, Jain M, Moore ED, et al. Pharmacokinetics and biodistribution of ¹⁷⁷Lu-labeled multivalent single-chain Fv construct of the pancarcinoma monoclonal antibody CC49. *Eur J Nucl Med Mol Imaging* 2005;32:264–273.
132. Adams GP, McCartney JE, Tai MS, et al. Highly specific *in vivo* tumor targeting by monovalent and divalent forms of 741F8 anti-c-erbB-2 single-chain Fv. *Cancer Res* 1993;53:4026–4034.
133. Adams GP, Tai MS, McCartney JE, et al. Avidity-mediated enhancement of *in vivo* tumor targeting by single-chain Fv dimers. *Clin Cancer Res* 2006;12:1599–1605.
134. Hu S, Shively L, Raubitschek A, et al. Minibody: A novel engineered anti-carcinoembryonic antigen antibody fragment (single-chain Fv-C_H3) which exhibits rapid, high-level targeting of xenografts. *Cancer Res* 1996;56:3055–3061.
135. Sundaresan G, Yazaki PJ, Shively JE, et al. ¹²⁴I-labeled engineered anti-CEA minibodies and diabodies allow high-contrast, antigen-specific small-animal PET imaging of xenografts in athymic mice. *J Nucl Med* 2003;44:1962–1969.
136. Wong JY, Chu DZ, Williams LE, et al. Pilot trial evaluating an ¹²³I-labeled 80-kilodalton engineered anticarcinoembryonic antigen antibody fragment (cT84.66 minibody) in patients with colorectal cancer. *Clin Cancer Res* 2004;10:5014–5021.
137. Olafsen T, Tan GJ, Cheung CW, et al. Characterization of engineered anti-p185HER-2 (scFv-C_H3)₂ antibody fragments (minibodies) for tumor targeting. *Protein Eng Des Sel* 2004;17:315–323.
138. Rose LM, Deng CT, Scott SL, et al. Critical Lym-1 binding residues on polymorphic HLA-DR molecules. *Mol Immunol* 1999;36:789–797.
139. Shi XB, Gumerlock PH, Kroger L, DeNardo GL, DeNardo SJ. Efficient recombination of Lym-1 scFv gene using multiple doubly-restricted DNA fragments. *Cancer Biother Radiopharm* 1999;14:139–143.
140. Balhorn R, Hok S, Burke PA, et al. Selective high-affinity ligand antibody mimics for cancer diagnosis and therapy: initial application to lymphoma/leukemia. *Clin Cancer Res* 2007;13:5621s–5628s.
141. DeNardo GL, Natarajan A, Hok S, et al. Pharmacokinetic characterization in xenografted mice of a series of first-generation mimics for HLA-DR antibody, Lym-1, as carrier molecules to image and treat lymphoma. *J Nucl Med* 2007;48:1338–1347.
142. Hok S, Natarajan A, Balhorn R, DeNardo SJ, DeNardo GL, Perkins J. Synthesis and radiolabeling of selective high-affinity ligands designed to target non-Hodgkin's lymphoma and leukemia. *Bioconjug Chem* 2007;18:912–921.
143. West J, Perkins J, Hok S, et al. Direct antilymphoma activity of novel, first-generation “antibody mimics” that bind HLA-DR10-positive non-Hodgkin's lymphoma cells. *Cancer Biother Radiopharm* 2006;21:645–654.
144. Nilsson B, Moks T, Jansson B, et al. A synthetic IgG-binding domain based on staphylococcal protein A. *Protein Eng* 1987;1:107–113.
145. Wikman M, Steffen AC, Gunneriusson E, et al. Selection and characterization of HER2/neu-binding affibody ligands. *Protein Eng Des Sel* 2004;17:455–462.
146. Steffen AC, Wikman M, Tolmachev V, et al. *In vitro* characterization of a bivalent anti-HER-2 affibody with potential for radionuclide-based diagnostics. *Cancer Biother Radiopharm* 2005;20:239–248.
147. Steffen AC, Orlova A, Wikman M, et al. Affibody-mediated tumour targeting of HER-2 expressing xenografts in mice. *Eur J Nucl Med Mol Imaging* 2006;33:631–638.

148. Orlova A, Tolmachev V, Pehrson R, et al. Synthetic affibody molecules: a novel class of affinity ligands for molecular imaging of HER2-expressing malignant tumors. *Cancer Res* 2007;67:2178–2186.
149. Orlova A, Magnusson M, Eriksson TL, et al. Tumor imaging using a picomolar affinity HER2 binding affibody molecule. *Cancer Res* 2006;66:4339–4348.
150. Orlova A, Rosik D, Sandstrom M, Lundqvist H, Einarsson L, Tolmachev V. Evaluation of [$^{111}/^{114m}\text{In}$]CHX-A''-DTPA-ZHER2:342, an affibody ligand conjugate for targeting of HER2-expressing malignant tumors. *Q J Nucl Med Mol Imaging* 2007; 51:314–323.
151. Tolmachev V, Xu H, Wallberg H, et al. Evaluation of a maleimido derivative of CHX-A'' DTPA for site-specific labeling of affibody molecules. *Bioconjug Chem* 2008.
152. Rodewald R. pH-dependent binding of immunoglobulins to intestinal cells of the neonatal rat. *J Cell Biol* 1976;71:666–669.
153. Kim JK, Firan M, Radu CG, Kim CH, Ghetie V, Ward ES. Mapping the site on human IgG for binding of the MHC class I-related receptor. *FcRn. Eur J Immunol* 1999; 29:2819–2825.
154. Ghetie V, Popov S, Borvak J, et al. Increasing the serum persistence of an IgG fragment by random mutagenesis. *Nat Biotechnol* 1997;15:637–640.
155. Kenanova V, Olafsen T, Crow DM, et al. Tailoring the pharmacokinetics and positron emission tomography imaging properties of anti-carcinoembryonic antigen single-chain Fv-Fc antibody fragments. *Cancer Res* 2005;65:622–631.
156. Kenanova V, Olafsen T, Williams LE, et al. Radioiodinated versus radiometal-labeled anti-carcinoembryonic antigen single-chain Fv-Fc antibody fragments: optimal pharmacokinetics for therapy. *Cancer Res* 2007;67:718–726.
157. Ferl GZ, Kenanova V, Wu AM, DiStefano JJ 3rd. A two-tiered physiologically based model for dually labeled single-chain Fv-Fc antibody fragments. *Mol Cancer Ther* 2006;5:1550–1558.
158. Wu AM, Tan GJ, Sherman MA, et al. Multimerization of a chimeric anti-CD20 single-chain Fv-Fc fusion protein is mediated through variable domain exchange. *Protein Eng* 2001;14:1025–1033.
159. Abuchowski A, McCoy JR, Palczuk NC, van Es T, Davis FF. Effect of covalent attachment of polyethylene glycol on immunogenicity and circulating life of bovine liver catalase. *J Biol Chem* 1977;252:3582–3586.
160. Bailon P, Palleroni A, Schaffer CA, et al. Rational design of a potent, long-lasting form of interferon: a 40 kDa branched polyethylene glycol-conjugated interferon alpha-2a for the treatment of hepatitis C. *Bioconjug Chem* 2001;12:195–202.
161. Wilkinson I, Jackson CJ, Lang GM, Holford-Strevens V, Sehon AH. Tolerogenic polyethylene glycol derivatives of xenogeneic monoclonal immunoglobulins. *Immunol Lett* 1987;15:17–22.
162. Takashina K, Kitamura K, Yamaguchi T, Noguchi A, Tsurumi H, Takahashi T. Comparative pharmacokinetic properties of murine monoclonal antibody A7 modified with neocarzinostatin, dextran and polyethylene glycol. *Jpn J Cancer Res* 1991; 82:1145–1150.
163. Lee LS, Conover C, Shi C, Whitlow M, Filpula D. Prolonged circulating lives of single-chain Fv proteins conjugated with polyethylene glycol: a comparison of conjugation chemistries and compounds. *Bioconjug Chem* 1999;10:973–981.

164. Li L, Yazaki PJ, Anderson AL, et al. Improved biodistribution and radioimmunoimaging with poly(ethylene glycol)-DOTA-conjugated anti-CEA diabody. *Bioconjug Chem* 2006;17:68–76.
165. Molineux G. Pegylation: engineering improved pharmaceuticals for enhanced therapy. *Cancer Treat Rev* 2002;28 Suppl A: 13–16.
166. Natarajan A, Xiong C, Albrecht H, DeNardo GL, DeNardo SJ. Characterization of site-specific ScFv PEGylation for tumor-targeting pharmaceuticals. *Bioconjug Chem* 2005;16:113–121.
167. Yang K, Basu A, Wang M, et al. Tailoring structure–function and pharmacokinetic properties of single-chain Fv proteins by site-specific PEGylation. *Protein Eng* 2003;16:761–770.
168. Xiong CY, Natarajan A, Shi XB, Denardo GL, Denardo SJ. Development of tumor targeting anti-MUC-1 multimer: effects of di-scFv unpaired cysteine location on PEGylation and tumor binding. *Protein Eng Des Sel* 2006;19:359–367.
169. Albrecht H, Denardo GL, Denardo SJ. Monospecific bivalent scFv-SH: effects of linker length and location of an engineered cysteine on production, antigen binding activity and free SH accessibility. *J Immunol Methods* 2006;310:100–116.
170. Kragh-Hansen U, Chuang VT, Otagiri M. Practical aspects of the ligand-binding and enzymatic properties of human serum albumin. *Biol Pharm Bull* 2002;25:695–704.
171. Chuang VT, Kragh-Hansen U, Otagiri M. Pharmaceutical strategies utilizing recombinant human serum albumin. *Pharm Res* 2002;19:569–577.
172. Smith BJ, Popplewell A, Athwal D, et al. Prolonged *in vivo* residence times of antibody fragments associated with albumin. *Bioconjug Chem* 2001;12:750–756.
173. Yazaki PJ, Kassa T, Cheung CW, et al. Biodistribution and tumor imaging of an anti-CEA single-chain antibody–albumin fusion protein. *Nucl Med Biol* 2008;35:151–158.
174. Tijink BM, Laeremans T, Budde M, et al. Improved tumor targeting of anti-epidermal growth factor receptor Nanobodies through albumin binding: taking advantage of modular Nanobody technology. *Mol Cancer Ther* 2008;7:2288–2297.
175. Dennis MS, Zhang M, Meng YG, et al. Albumin binding as a general strategy for improving the pharmacokinetics of proteins. *J Biol Chem* 2002;277:35035–35043.
176. Dennis MS, Jin H, Dugger D, et al. Imaging tumors with an albumin-binding Fab, a novel tumor-targeting agent. *Cancer Res* 2007;67:254–261.
177. Nguyen A, Reyes AE, 2nd Zhang M, et al. The pharmacokinetics of an albumin-binding Fab (AB.Fab) can be modulated as a function of affinity for albumin. *Protein Eng Des Sel* 2006;19:291–297.